Vickers indentation fracture toughness test Part 2 Application and critical evaluation of standardised indentation toughness equations

The standardised indentation fracture toughness equations formulated in Part 1 have been applied to a range of brittle materials: namely, glass ceramics, aluminas, zirconias, and WC–Co cermets. Analysis of the results has enabled a critical assessment of (i) the ability of the nineteen equations to yield the same fracture toughness values as a conventional fracture toughness test and (ii) their ability to rank materials in order of fracture toughness. Also, specific equations have been recommended as being the most appropriate equations to use.

MST/1050b

C. B. Ponton
R. D. Rawlings

 Manuscript received 7 February 1989; in final form 6 June 1989. *At the time the work was carried out the authors were in the Department of Materials, Imperial College of Science, Technology and Medicine, London. Dr Ponton is now is the School of Metallurgy and Materials, The University of Birmingham.*

Introduction

The relative merits of the 19 standardised Vickers indentation fracture toughness equations given in Part 1[1] are assessed by using the indenter load data together with the indentation half-diagonal and crack length data for two aluminas, seven Silceram glass ceramics in the system $CaO–MgO–Al_2O_3–SiO_2$, four tetragonal zirconia polycrystals (TZPs), a zirconia toughened alumina (ZTA), and two cobalt bonded tungsten carbide cermets. The resulting toughness values are compared with the values obtained from conventional fracture toughness tests such as the single edge notched beam (SENB) test. However, before evaluating the equations, the effect on the crack length of factors other than the inherent fracture toughness of the material is discussed, together with the techniques that can be used to measure the crack lengths.

Surface radial crack length

FACTORS AFFECTING SURFACE CRACK LENGTH

A number of factors can prevent the actual measurement of the radial or Palmqvist surface crack lengths or render the measured values invalid.

The first factor to be considered is the surface stress state before indentation, which may be inadvertently neglected when applying the Vickers indentation test. The apparent surface crack length is a reflection of both the fracture toughness of the material and any pre-existing surface stresses, be they compressive or tensile. All the Vickers indentation fracture models in Part 1[1] are based on the assumption that there are no pre-existing surface stresses.

A compressive surface stress will decrease the surface crack length relative to the equilibrium length in the absence of surface stresses;[2] a tensile stress will do the reverse. Surface stresses may be induced in a number of ways, such as mechanical damage, thermal tempering, ion exchange, and ion bombardment. For example, mechanical damage due to surface grinding, a common processing step for ceramics, produces a compressive surface stress.[2–5]

For the great majority of materials to which the Vickers indentation test can be applied, the process of polishing the specimen (to produce a plane, highly reflective test surface) reduces and, it is hoped, removes any surface stresses caused by earlier surface finishing processes such as grinding. However, this should not be taken for granted; the early work on cermets (*see* 'Origins of Vickers indentation toughness test' in Part 1[1]) serves as a reminder that the surface stress state must always be considered (e.g. *see* Ref. 6).

Second, the initiation and propagation of subsurface lateral cracks, sideways away from the base of the indentation plastic zone and roughly parallel to the specimen surface just before and on unloading of the indenter,[7–10] can also affect the surface crack length. Lateral cracks continue to extend after complete unloading under the action of the irreversible residual crack mouth opening matrix stress field,[11,12] arcing towards the specimen surface. Thus, they often intersect the surface resulting in the removal of surface material from within one or more of the regions bounded by the surface cracks, obliterating any trace of the said surface cracks along most of their length. The extent of lateral cracking is greater in harder materials,[8] and the incidence of consequent gross chipping or spalling usually increases with increasing indenter load.[13,14]

Both the growth and breakthrough of lateral cracks to the surface relaxes the constraint exerted by the elastic matrix on the indentation plastic zone, which reduces the magnitude of the residual stress field.[15] This has been shown to result in crack tip closure of the median crack and the surviving lateral crack of a Knoop indentation in soda–lime silicate glass.[16] This tip closure prevents the cracks attaining their postindentation equilibrium lengths for a given indenter load; thus, even if the crack tips of the bounding cracks are visible, the use of such crack length data is likely to overestimate the fracture toughness of the material.

A third factor, is the occurrence of environmentally assisted, time dependent postindentation slow crack growth in susceptible materials such as silicate glasses,[17–19] which is initiated by the residual stress field operating during and after unloading. All three types of indentation crack, i.e. radial surface, median, and lateral, can experience slow crack growth. The slow crack growth of any lateral cracks will lead to a reduction in the residual stress field, thereby

countering the simultaneous slow crack growth of the radial and median cracks. Furthermore, severe chipping at high indenter loads may be expected to release all constraints on the indentation plastic zone, essentially reducing the residual stress field to zero; in this case, no slow crack growth would be expected.[16]

Thus, the observation by Anstis *et al.*[18] that post-indentation slow crack growth of the lateral cracks in soda–lime silicate glass in an oil environment ultimately allowed the lateral crack fronts to catch up with the radial–median crack fronts might also be interpreted as the slow crack growth of the lateral cracks reducing the simultaneous slow crack growth rate of the radial–median crack system by relaxing the residual stress field.

If slow crack growth occurs, the measured crack lengths will possess a systematic error and the indentation toughness K_c data from all indentation toughness equations will be equally affected. Thus, it is advisable to monitor the mean radial or Palmqvist surface crack lengths of a number of indents, as well as the initiation and propagation of any concomitant lateral cracks, as a function of time after indenter unloading, for example, as soon as possible after unloading and 1 h, 12 h, and 1 day later. This will indicate (i) the sensitivity of the material to postindentation slow crack growth and (ii) how quickly the crack length should be measured after indentation for the measured lengths to be taken as the equilibrium values such that $K \equiv K_c$. If the material is sensitive to slow crack growth, a ln–ln plot of the surface crack length versus elapsed time data may be used to determine the K_c value by extrapolation back to zero elapsed time.[18,19]

The last factor to be considered is the effect of microstructure on indentation crack morphology. When annealed soda–lime silicate glass is indented, the radial surface cracks emanating from the corners of a Vickers indent are equal in length and the indentation itself is equiaxial along the diagonals as a result of the isotropic structure of the glass.[20] However, in brittle polycrystalline materials, the microstructure affects the indentation cracks in a number of ways, such as crack termination at porosity and/or grain boundaries normal to the crack path and crack deflection along grain boundaries.[21]

The effect of the microstructure depends on the size and density of the dominant microstructural features relative to the indent size. Thus, if the average grain size is very much greater than the indent size (i.e. $\gg 2a$) an indent in a grain will give a toughness similar to the single crystal toughness. However, indents at grain boundary intersections or on grain boundaries will give anomalous toughness data. When the mean grain size is much smaller than $2a$ the indent crack morphology will be reminiscent of that in soda–lime glass, except for the asymmetric crack lengths and the undulating indent edges and cracks which follow the grain boundaries.[13,18,21] Thus, the measured toughness will represent the polycrystal toughness.

For a mean grain size similar to $2a$, Anstis *et al.*[18] noted that when Coors Vistal alumina (grain size 20 μm) and Coors AD999 alumina (grain size 3 μm) were indented at a load of 50 N (producing in both ceramics indent diagonal lengths of $\sim$80 μm), the former suffered crack pattern disruption in the form of discontinuous and multiple cracks emanating from the indentation corners, as well as cracks emerging from the sides of the indentation rather than from the corners, while the latter did not. Evans[22] has reported severe crack pattern disruption in relatively coarse grained ($\geqslant \sim 20$ μm grain size) ceramics sintered to full density (translucency) with the aid of specific additives, e.g. alumina sintered with MgO (General Electric Lucalox), as have Smith and Pletka.[21] Thus, when the grain size is of the order of $2a$, the indent crack pattern is likely to be severely disrupted by localised grain fracture events and as a result the Vickers indentation toughness test cannot be used with any confidence, or indeed, validity.

A final point to note is that the elastic–plastic stress field generated by an indentation should not interact with the stress field of any adjacent indentations nor be subject to modification by adjacent free surfaces, i.e. surfaces beneath or perpendicular to the indented surface. It is suggested that the specimen thickness should be at least an order of magnitude greater than $\sim 2c$ and that adjacent indent centres should be no closer than $\sim 4c$ (where c is the surface radial crack length).

MEASUREMENT OF SURFACE CRACK LENGTH

To measure the radial (or Palmqvist) surface crack lengths the specimen test surface must be polished before indentation until it is optically reflective. This invariably requires polishing using diamond pastes through to 1 μm at least. In some instances, a finer finish is required, e.g. polishing with 0·05 μm Al_2O_3. Even after polishing, diffuse scattering of incident light may make difficult the optical observation of the surface cracks. However, the test surface can be coated with a vacuum sputtered layer of gold or gold alloy ($\sim$20 to 40 nm thick) to eliminate any diffuse scattering of incident light, enabling the crack lengths to be measured more accurately. The authors consider that coating the surface with gold before (rather than after) indentation is to be preferred, because the coating process may affect the postindentation crack length and the gold film is likely to obscure optically the crack tips. A further advantage of precoating with gold is that the slight surface displacement accompanying surface cracking will rupture the gold film making the surface cracks more visible.

An alternative method of highlighting the surface cracks is to use a dye penetrant (fluorescent or otherwise), particularly on opaque ceramics which are light in colour, e.g. alumina, zirconia. The authors have successfully used various dye penetrants on these materials. However, it must be remembered that their use after indentation is likely to enhance postindentation slow crack growth in many glasses, glass ceramics, and ceramics. In transluscent materials, the full extent of the cracks can be determined by using dark field or angled illumination; for transparent materials, transmitted light can also be used.

There is a number of ways in which the crack lengths can be measured, the most convenient being direct optical measurement using a calibrated eyepiece graticule. With this method, it is difficult to measure the true length of an undulating crack and hence the crack length l is invariably measured as the straight length from the corner of the indentation to the crack tip which may result in a measurement error. However, by taking optical negatives of the indentation–crack system at calibrated magnifications, from which enlarged micrographs can be made, the accuracy of the measurement can be increased. More accurate optical crack length measurements, employing optical interference contrast, i.e. optical interferometry, are possible because of the small surface displacement which accompanies any surface crack. Last, the high topographical resolution of a scanning electron microscope (SEM) enables highly accurate crack length measurements to be taken from calibrated, enlarged micrographs of the indent–crack system.

However, given the time and expense involved in taking optical or SEM micrographs, the crack length measurements are most likely to be made by direct optical microscopy. Thus, the authors have investigated the relative accuracy of direct optical and SEM crack length measurements for Vickers indentations in cast Silceram SCF5. A calibrated JEOL T200 SEM and a calibrated Reichert optical microscope were used for the SEM and optical measurements, respectively. In Table 1, crack length measurements taken from SEM negatives of indents made

at 152, 148, and 103 N are compared with the corresponding optical crack length measurements. As would be expected the crack lengths determined using SEM were longer than the optically determined crack lengths; however, the difference was no more than ~4%.

A similar comparison by Petrovic,[23] using Corning Pyroceram C9606 glass ceramic (which has been employed by ASTM Subcommittee E 24.07 addressing 'Fracture mechanics test methods for brittle, non-metallic materials' for a comparison of the main fracture mechanics test methods for ceramic materials), showed that for 58·84 and 9·81 N Vickers indentations the calibrated crack lengths measured using SEM exceeded the measured crack lengths obtained from calibrated optical micrographs by about 4 and 15%, respectively. Thus, it appears that surface crack lengths can be measured optically with acceptable accuracy when indentation loads of $\geqslant 50$ N are employed.

Experimental procedure and results

EXPERIMENTAL PROCEDURE

Specimen preparation

All the materials used by the authors and their colleagues for the indentation tests, namely, the cast and hot press sintered Silceram glass ceramics, the Vitox biograde alumina (manufactured by Morgan Matroc Ltd, Anderman Division), the three yttria stabilised TZP materials (coded A, B, and C), and the yttria stabilised ZTA material, were prepared for indentation testing by carefully diamond polishing the test surface, finishing with 1 or 0·25 μm grade diamond. The final polished surface was then vacuum coated with gold.

Indenting procedure

The hot press sintered Silceram materials and the cast Silceram materials SCR19.34 and SCR25.76 were indented using a standard Vickers macrohardness testing machine with a load of 5 kgf (49 N). The other materials were indented for a nominal period of 15 s using a Vickers indenter fixed to the crosshead of a table-top universal testing machine; the crosshead speed was fixed at 0·5 mm min^{-1}. The number of indents made in a material ranged from 6 to 33. The TZP materials (A, B, and C) and the cast Silceram SCR19.13 were indented at a nominal load of 60 N, while the Vitox alumina, the ZTA material, and the cast Silceram SCF5 were indented at a nominal load of 50 N. Silceram SCF5 was also indented at nominal loads of 100 and 150 N to investigate the effect of indenter load on indentation fracture.

Surface crack length measurement

The Palmqvist crack lengths and the indentation half-diagonal lengths were measured directly using a Reichert or Leitz optical microscope with a calibrated eyepiece graticule and a magnification appropriate to the size of the indents: typically, ×450 or ×500. The average radial surface crack length, average Palmqvist crack length, and average half-diagonal length were used in the indentation fracture toughness equations.

Table 1 Comparison of crack lengths measured using scanning electron microscopy (SEM) and optical microscopy (OM) of Vickers indentations in Silceram glass ceramic SCF5

	Mean crack length, μm, measured using	
Indenter load, N	SEM	OM
152	392	375
148	386	379
103	332	326

Crack profile characterisation

An assessment was made of the nature of the Vickers indentation crack profiles produced in the cast and hot press sintered Silceram glass ceramics, and Vitox alumina, TZP (A, B, C), and ZTA ceramics under specified conditions. The profiles were determined by the serial polishing away of Vickers indents using a 1 μm diamond lapping wheel and observing the surface crack patterns.

The surface radial crack lengths of the cast Silcerams were mapped as a function of depth below the original surface. One sample of each cast Silceram, i.e. SCF5, SCR19.34, SCR19.13, and SCR25.76, was polished until the original indent had disappeared. The SCR19.34 sample was then polished further until the indentation cracks also disappeared. The depth of material removed was monitored by the changes in the diagonal dimensions of Vickers marker indents made in the vicinity of the indent being mapped. The marker indents were made at a load different from that of the mapped indent to ascertain the effect of indenter load on the crack profile. There was no difference between the crack profiles produced at 25 and 49 N; higher loads were not used, because of the risk of lateral crack breakthrough to the specimen surface.

The crack profiles in the sintered Silcerams, Vitox alumina, TZP, and ZTA ceramics were inferred from the surface crack patterns observed as the Vickers indents were polished away to the point at which they had all but disappeared. The indents in the Silcerams were made at 49 N, whereas those in the alumina, TZP, and ZTA ceramics were made at 10 kgf (98·1 N).

EXPERIMENTAL RESULTS

Vickers indentation fracture toughness data

The indentation toughness K_c data for the cast Silceram glass ceramics are given in Table 2; the values of the parameters important in indentation fracture, E/H_V, c/a, $P/c^{3/2}$, and P/l are also tabulated as also are the three point SENB K_{Ic} fracture toughness values. The mean K_c values are given for all the halfpenny model and Palmqvist model equations together with the ratios K_c/K_{Ic} (designated by σ). All mean values are quoted together with the sample standard deviations. The coefficients of variation of E, H_V, K_{Ic}, c/a, $P/c^{3/2}$, P/l, and E/H_V are also given when calculable, as an aid to assessing the contribution of each parameter to the variation in K_c.

This presentation style is also used in Tables 3–5; the data for the hot press sintered Silceram glass ceramics are tabulated in Table 3 and the data for TZP A, TZP B, TZP C and the ZTA are given in Table 4. The indentation toughness results derived from the data reported by Jones *et al.*[28] for an yttria stabilised TZP ceramic and an alumina ceramic, and by Laugier[29] for two WC–Co cermets, are given in Table 5 and refer to halfpenny cracks in alumina and Palmqvist cracks in the TZP ceramics and the WC–Co cermets.

Serial polishing results

In Figs. 1*a* and 1*b*, schematic diagrams are shown for *idealised* halfpenny and Palmqvist crack systems, respectively, after serial polishing down to a plane AA. However, it was found that the SCR19.34 sample had developed Palmqvist type cracks of the form shown schematically in Fig. 1*c*: the ratio of the crack depth to the Palmqvist crack length d/l, was ~1·8. The other cast Silcerams were found to have similar crack profiles down to the indent depth; therefore, presumably they have crack depths of the same

Table 2 Mean Vickers indentation fracture toughness K_c, MN m$^{-3/2}$, and K_c/K_{Ic} ratios (designated by σ) for cast Silceram glass ceramics SCF5, SCR19.34, SCR19.13, and SCR25.76

Material	SCF5		SCR19.34		SCR19.13		SCR25.76	
VALUES OF PARAMETERS* IMPORTANT IN INDENTATION FRACTURE								
E†, GN m^{-2}	120·6±0·9 (1%)		115·0±0·2 (0·2%)		100·6		121·7±1·5 (1%)	
H_V, GN m^{-2}	7·02±0·23 (3%)		7·34±0·08 (1%)		6·96±0·35 (5%)		7·47±0·13 (2%)	
K_{Ic}‡, MN m$^{-3/2}$	2·02±0·11 (5%)		1·83±0·06 (3%)		1·06±0·11 (11%)		2·29±0·21 (9%)	
c/a	3·61±0·29 (8%)		3·58±0·10 (3%)		4·86±0·44 (9%)		3·79±0·10 (3%)	
$P/c^{3/2}$, MN m$^{-3/2}$	19·3±2·1 (11%)		17·5±0·7 (4%)		11·1±1·4 (13%)		16·3±0·7 (4%)	
P/l, MN m^{-1}	0·45±0·08 (18%)		0·34±0·01 (3%)		0·24±0·03 (13%)		0·32±0·02 (3%)	
E/H_V	17·18		15·67		14·45		16·29	
VALUES OF K_c AND σ OBTAINED USING HALFPENNY MODELS								
Model[1]	K_c	σ	K_c	σ	K_c	σ	K_c	σ
LS	0·70±0·06	0·35	0·63±0·01	0·34	0·54±0·03	0·51	0·62±0·01	0·27
LF	1·00±0·11	0·50	0·90±0·04	0·49	0·57±0·07	0·54	0·84±0·04	0·37
EW	0·99±0·30	0·49	0·93±0·11	0·51	−0·30±0·37§	−0·28§	0·71±0·11	0·31
EC	1·59±0·17	0·79	1·44±0·06	0·79	0·92±0·11	0·87	1·34±0·06	0·59
ED	1·93±0·20	0·96	1·69±0·07	0·92	1·03±0·11	0·97	1·59±0·07	0·69
B	2·13±0·19	1·05	1·86±0·06	1·02	1·16±0·18	1·09	1·78±0·06	0·78
LEM	1·07±0·11	0·53	0·93±0·04	0·51	0·57±0·07	0·54	0·88±0·04	0·38
ACLM	1·23±0·13	0·61	1·07±0·04	0·58	0·65±0·08	0·61	1·01±0·04	0·44
NMH1	1·99±0·21	0·99	1·73±0·07	0·95	1·07±0·13	1·01	1·64±0·07	0·72
JL	2·03±0·22	1·00	1·77±0·07	0·97	1·07±0·14	1·01	1·66±0·07	0·72
MM1	2·03±0·22§	1·00§	1·62±0·03§	0·89§	1·24±0·08§	1·17§	1·68±0·03§	0·73§
MM2	1·73±0·18	0·86	1·39±0·04	0·76	0·90±0·10	0·85	1·39±0·04	0·61
L1	1·22±0·13	0·60	1·04±0·04	0·57	0·63±0·08	0·59	0·99±0·04	0·43
L2	1·33±0·14	0·66	1·16±0·05	0·63	0·71±0·09	0·67	1·09±0·04	0·48
T	1·38±0·15	0·68	1·22±0·05	0·67	0·76±0·09	0·72	1·14±0·05	0·50
VALUES OF K_c AND σ OBTAINED USING PALMQVIST MODELS								
Model[1]	K_c	σ	K_c	σ	K_c	σ	K_c	σ
NMH2	2·27±0·20§	1·12§	1·97±0·04§	1·08§	1·56±0·09§	1·47§	1·95±0·04§	0·85§
N	3·12±0·28§	1·54§	2·70±0·05§	1·48§	2·14±0·13§	2·02§	2·67±0·05§	1·17§
SWMC	2·61±0·22	1·29	2·35±0·04	1·28	1·92±0·13	1·81	2·29±0·05	1·00
L3	1·15±0·18	0·57	0·98±0·06	0·54	0·49±0·09	0·46	0·90±0·05	0·39

* E is Young's modulus, H_V is Vickers hardness, K_{Ic} is fracture toughness, c is radial crack length, a is indentation half-diagonal length, P is test load, and l is Palmqvist crack length. Coefficients of variation are given in parentheses.
† These data were measured experimentally using Förster's forced resonance method.[24]
‡ These values were determined by conventional three point bending SENB plane strain fracture toughness tests.
§ These K_c and σ values are not valid because the c/a or l/a limits of the equations are not satisfied.

Table 3 Mean Vickers indentation fracture toughness K_c, MN m$^{-3/2}$, and K_c/K_{Ic} ratios (designated by σ) for Vitox alumina and hot press sintered Silceram glass ceramics SCR19.34 HPC2, HPC3, and HPC4

Material	Vitox		SCR19.34 HPC2		SCR19.34 HPC3		SCR19.34 HPC4	
VALUES OF PARAMETERS* IMPORTANT IN INDENTATION FRACTURE								
E†, GN m^{-2}	400		120		120		120	
H_V, GN m^{-2}	19·21±0·97 (5%)		6·24±1·07 (17%)		6·54±1·08 (17%)		6·94±1·19 (17%)	
K_{Ic}‡, MN m$^{-3/2}$	6·02±0·68 (11%)		2·36±0·16 (7%)		2·42±0·10 (4%)		2·51±0·13 (5%)	
c/a	2·96±0·22 (7%)		2·52±0·33 (13%)		2·33±0·31 (13%)		2·25±0·26 (12%)	
$P/c^{3/2}$, MN m$^{-3/2}$	48·3±4·9 (10%)		26·8±6·1 (23%)		31·0±5·5 (18%)		33·9±5·8 (17%)	
P/l, MN m^{-1}	0·74±0·08 (11%)		0·56±0·14 (25%)		0·65±0·14 (22%)		0·71±0·15 (21%)	
E/H_V	20·82		19·23		18·35		17·29	
VALUES OF K_c AND σ OBTAINED USING HALFPENNY MODELS								
Model[1]	K_c	σ	K_c	σ	K_c	σ	K_c	σ
LS	1·43±0·05	0·24	0·67±0·09	0·28	0·72±0·07	0·30	0·76±0·08	0·30
LF	2·49±0·25	0·41	1·38±0·31	0·58	1·60±0·28	0·66	1·75±0·30	0·70
EW	3·53±0·58	0·59	2·10±0·51	0·89	2·44±0·44	1·01	2·68±0·42	1·07
EC	3·98±0·40	0·66	2·21±0·50	0·94	2·55±0·45	1·05	2·79±0·48	1·11
ED	5·08±0·43	0·84	2·47±0·30	1·05	2·67±0·23	1·10	2·80±0·20	1·12
B	5·26±0·36	0·87	2·52±0·30	1·07	2·73±0·24	1·13	2·85±0·23	1·14
LEM	2·96±0·32	0·49	1·58±0·33	0·67	1·79±0·33	0·74	1·90±0·33	0·76
ACLM	3·40±0·37	0·56	1·81±0·38	0·77	2·06±0·38	0·85	2·19±0·38	0·87
NMH1	5·38±0·58	0·89	2·89±0·61	1·22	3·30±0·59§	1·36§	3·52±0·59§	1·40§
JL	5·55±0·62	0·92	3·01±0·66	1·28	3·45±0·64	1·43	3·69±0·65	1·47
MM1	5·22±0·29§	0·87§	2·22±0·23	0·94	2·26±0·27	0·93	2·23±0·27	0·89
MM2	5·02±0·48	0·83	2·36±0·40§	1·00§	2·53±0·47§	1·05§	2·54±0·46§	1·01§
L1	3·48±0·39	0·58	1·84±0·38	0·78	2·07±0·39	0·86	2·18±0·39	0·87
L2	3·59±0·38	0·60	1·93±0·40	0·82	2·20±0·39	0·91	2·34±0·40	0·93
T	3·62±0·38	0·60	1·97±0·42	0·83	2·25±0·40	0·93	2·43±0·40	0·97
VALUES OF K_c AND σ OBTAINED USING PALMQVIST MODELS								
Model[1]	K_c	σ	K_c	σ	K_c	σ	K_c	σ
NMH2	5·25±0·29	0·87	2·50±0·31	1.06	2·71±0·28	1·12	2·85±0·30	1·14
N	7·19±0·39	1·19	3·42±0·43	1.45	3·72±0·39	1·54	3·90±0·41	1·55
SWMC	5·58±0·29	0·93	2·74±0·44	1.16	3·03±0·37	1·25	3·25±0·41	1·29
L3	3·79±0·63	0·63	2·33±0·80	0.99	2·82±0·85	1·17	3·03±0·92	1·21

* E is Young's modulus, H_V is Vickers hardness, K_{Ic} is fracture toughness, c is radial crack length, a is indentation half-diagonal length, P is test load, and l is Palmqvist crack length. Coefficients of variation are given in parentheses.
† The value for Vitox is after Real *et al.*;[25] the values for the hot press sintered Silceram glass–ceramics, SCR19.34 HPC2, HPC3 and HPC4, are estimates calculated by Kim.[26]
‡ The values were determined by conventional three point bending SENB plane strain fracture toughness tests.
§ These K_c and σ values are not valid because the c/a or l/a limits of the equations are not satisfied.

Table 4 Mean Vickers indentation fracture toughness K_c, MN m$^{-3/2}$, and K_c/K_{Ic} ratios (designated by σ) for TZP materials A, B, and C, and ZTA material

Material	TZP A		TZP B		TZP C		ZTA	
VALUES OF PARAMETERS* IMPORTANT IN INDENTATION FRACTURE								
E†, GN m^{-2}	210		210		210		340	
H_V, GN m^{-2}	13·14±0·58 (5%)		12·85±1·22 (10%)		13·33±0·59 (5%)		14·89±1·10 (7%)	
K_{Ic}‡, MN m$^{-3/2}$	9·43±1·33 (14%)		10·76±1·17 (11%)		10·73±0·81 (8%)		6·5±0·3 (5%)	
c/a	1·60±0·19 (12%)		1·64±0·18 (11%)		1·86±0·26 (14%)		1·53±0·10 (7%)	
$P/c^{3/2}$, MN m$^{-3/2}$	96·8±14·0 (15%)		91·5±12·3 (13%)		79·8±15·7 (20%)		108·0±11·8 (11%)	
P/l, MN m^{-1}	2·44±0·95 (39%)		2·16±0·59 (27%)		1·68±0·46 (27%)		2·50±0·48 (19%)	
E/H_V	15·98		16·34		15·75		22·83	
VALUES OF K_c AND σ OBTAINED USING HALFPENNY MODELS								
Model[1]	K_c	σ	K_c	σ	K_c	σ	K_c	σ
LS	1·54±0·05	0·16	1·50±0·10	0·14	1·46±0·12	0·14	1·66±0·10	0·26
LF	4·99±0·72	0·53	4·71±0·63	0·44	4·11±0·81	0·38	5·56±0·61	0·86
EW	6·85±0·49	0·73	6·57±0·56	0·61	6·01±0·96	0·56	7·52±0·59	1·16
EC	7·98±1·16	0·85	7·54±1·01	0·70	6·58±1·30	0·61	8·90±0·97	1·37
ED	5·60±0·18	0·59	5·49±0·21	0·51	5·26±0·43	0·49	6·92±0·26	1·06
B	5·94±0·24	0·63	5·81±0·26	0·54	5·49±0·53	0·51	7·39±0·33	1·14
LEM	5·20±0·84	0·55	4·97±0·69	0·46	4·24±0·81	0·40	6·92±0·69	1·06
ACLM	5·97±0·97	0·63	5·71±0·79	0·53	4·88±0·93	0·45	7·95±0·80	1·22
NMH1	9·70±1·54§	1·03§	9·25±1·26§	0·86§	7·93±1·52§	0·74§	12·46±1·26§	1·92§
JL	10·93±1·74	1·10	9·88±1·41	0·92	8·42±1·67	0·78	13·37±1·40	2·06
MM1	4·07±0·25	0·43	4·07±0·32	0·38	3·77±0·27	0·35	6·67±0·31	1·03
MM2	5·61±0·76§	0·59§	5·54±0·72§	0·51§	4·79±0·66§	0·45§	9·41±0·74§	1·45§
L1	5·86±0·99	0·62	5·62±0·80	0·52	4·76±0·90	0·44	8·27±0·83	1·27
L2	6·47±1·03	0·69	6·16±0·84	0·57	5·29±1·01	0·49	8·31±0·84	1·28
T	6·78±1·04	0·72	6·44±0·87	0·60	5·56±1·08	0·52	8·27±0·85	1·27
VALUES OF K_c AND σ OBTAINED USING PALMQVIST MODELS								
Model[1]	K_c	σ	K_c	σ	K_c	σ	K_c	σ
NMH2	6·98±1·22	0·74	6·61±0·83	0·61	5·84±0·83	0·54	8·78±0·86	1·35
N	9·57±1·67§	1·01§	9·03±1·14§	0·84§	8·00±1·14§	0·75§	12·03±1·18§	1·85§
SWMC	8·24±1·31	0·87	7·74±0·98	0·72	6·95±1·04	0·65	9·00±0·95	1·38
L3	12·29±5·12	1·30	11·08±3·37	1·03	8·14±2·50	0·76	17·50±3·40	2·69

* E is Young's modulus, H_V is Vickers hardness, K_{Ic} is fracture toughness, c is radial crack length, a is indentation half-diagonal length, P is test load, and l is Palmqvist crack length. Coefficients of variation are given in parentheses.
† The values given were supplied by the manufacturer; the values given by the manufacturer for the TZP materials are similar to the values reported in the literature for such materials. Measurements derived from Knoop hardness tests on TZP A, using the method of Marshall *et al.*,[27] gave $E = 199 \pm 29$ GN m^{-2}.
‡ The values were determined by conventional three point bending SENB plane strain fracture toughness tests.
§ These K_c and σ values are not valid because the c/a or l/a limits of the equations are not satisfied.

Table 5 Mean Vickers indentation fracture toughness K_c, MN m$^{-3/2}$, and K_c/K_{Ic} ratios (designated by σ) from TZP and Al_2O_3 data of Jones *et al.*[28] and WC–Co (vol.-%) data of Laugier[29]

Material	TZP	Al_2O_3	WC–5Co	WC–24Co
VALUES OF PARAMETERS* IMPORTANT IN INDENTATION FRACTURE				
E†, GN m^{-2}	210	350	640	551
H_V, GN m^{-2}	13·15±1·33 (10%)	17·01±2·05 (12%)	19·36±0·18 (1%)	13·44±0·07 (1%)
K_{Ic}‡, MN m$^{-3/2}$	5·5±0·7 (13%)	3	8·8	11·5
c/a	2·26±0·48 (21%)	4·23±0·49 (12%)	3·07±0·20 (7%)	1·29±0·09 (7%)
$P/c^{3/2}$, MN m$^{-3/2}$	65·7±7·0 (11%)	35·4±3·7 (10%)	76·3±3·9 (5%)	212·0±14·7 (7%)
P/l, MN m^{-1}	1·40±0·15 (11%)	0·82±0·28 (34%)	1·94±0·05 (3%)	12·1±2·8 (23%)
E/H_V	15·78	20·58	33	41
VALUES OF K_c AND σ OBTAINED USING HALFPENNY MODELS				
Model[1]	K_c σ	K_c σ	K_c σ	K_c σ
LS	1·48±0·21 0·27	1·52±0·26 0·51	2·36±0·05 0·27	2·76±0·10 0·24
LF	3·38±0·36 0·61	1·82±0·19 0·61	3·93±0·20 0·45	10·94±0·76 0·95
EW	5·06±0·39 0·92	0·53±0·93§ 0·18§	5·35±0·66 0·61	13·30±0·52 1·16
EC	5·42±0·58 0·99	2·92±0·30 0·97	6·29±0·32 0·71	17·50±1·21 1·52
ED	5·14±0·52 0·93	3·75±0·47 1·25	9·76±0·32 1·11	14·56±0·56 1·27
B	5·27±0·45 0·96	4·29±0·57 1·43	10·21±0·19 1·16	15·74±0·60 1·37
LEM	3·50±0·37 0·64	2·15±0·29 0·72	5·87±0·29 0·67	18·23±1·29 1·59
ACLM	4·03±0·42 0·73	2·48±0·33 0·83	6·75±0·33 0·77	20·95±1·48 1·82
NMH1	6·55±0·68§ 1·19§	3·92±0·49 1·31	10·20±0·50 1·16	30·96±2·18§ 2·69§
JL	6·87±0·81 1·25	3·95±0·49 1·32	10·49±0·56 1·19	33·55±2·47 2·92
MM1	3·83±0·66 0·70	5·42±1·20§ 1·81§	13·88±0·34§ 1·58§	19·92±0·78 1·73
MM2	4·32±0·43§ 0·79§	4·22±0·83 1·41	13·03±0·28 1·48	30·90±1·55§ 2·69§
L1	3·94±0·43 0·72	2·53±0·37 0·84	7·46±0·36 0·85	24·00±1·70 2·09
L2	4·36±0·45 0·79	2·61±0·33 0·87	6·80±0·34 0·77	20·64±1·45 1·79
T	4·59±0·47 0·83	2·64±0·30 0·88	6·40±0·32 0·73	18·81±1·31 1·64
VALUES OF K_c AND σ OBTAINED USING PALMQVIST MODELS				
Model[1]	K_c σ	K_c σ	K_c σ	K_c σ
NMH2	5·36±0·28 0·97	5·12±0·84§ 1·71§	10·27±0·14 1·17	23·17±2·67 2·01
N	7·35±0·38 1·34	7·02±1·15§ 2·34§	14·08±0·19 1·60	31·76±3·67§ 2·76§
SWMC	6·37±0·38 1·16	5·48±0·85 1·83	9·09±0·13 1·03	18·80±2·15 1·63
L3	5·71±2·09 1·04	2·14±0·35 0·71	7·84±0·77 0·89	69·40±14·65 6·03

* E is Young's modulus, H_V is Vickers hardness, K_{Ic} is fracture toughness, c is radial crack length, a is indentation half-diagonal length, P is test load, and l is Palmqvist crack length. Coefficients of variation are given in parentheses.
† The assumed TZP value is similar to the literature values quoted for such materials; the assumed alumina value was calculated by presuming $E/H_V \approx 20$–21; the WC–Co values were derived from the Laugier[29] E/H_V data.
‡ Jones *et al.*[28] quoted $K_{Ic} = 5$–6 MN m$^{-3/2}$ for the alumina; the WC–5Co K_{Ic} value is that reported by Chermant and Osterstock,[30] and the WC–24Co K_{Ic} value was estimated from Fig. 3 of Ref. 30.
§ These K_c and σ values are not valid because the c/a or l/a limits of the equations are not satisfied.

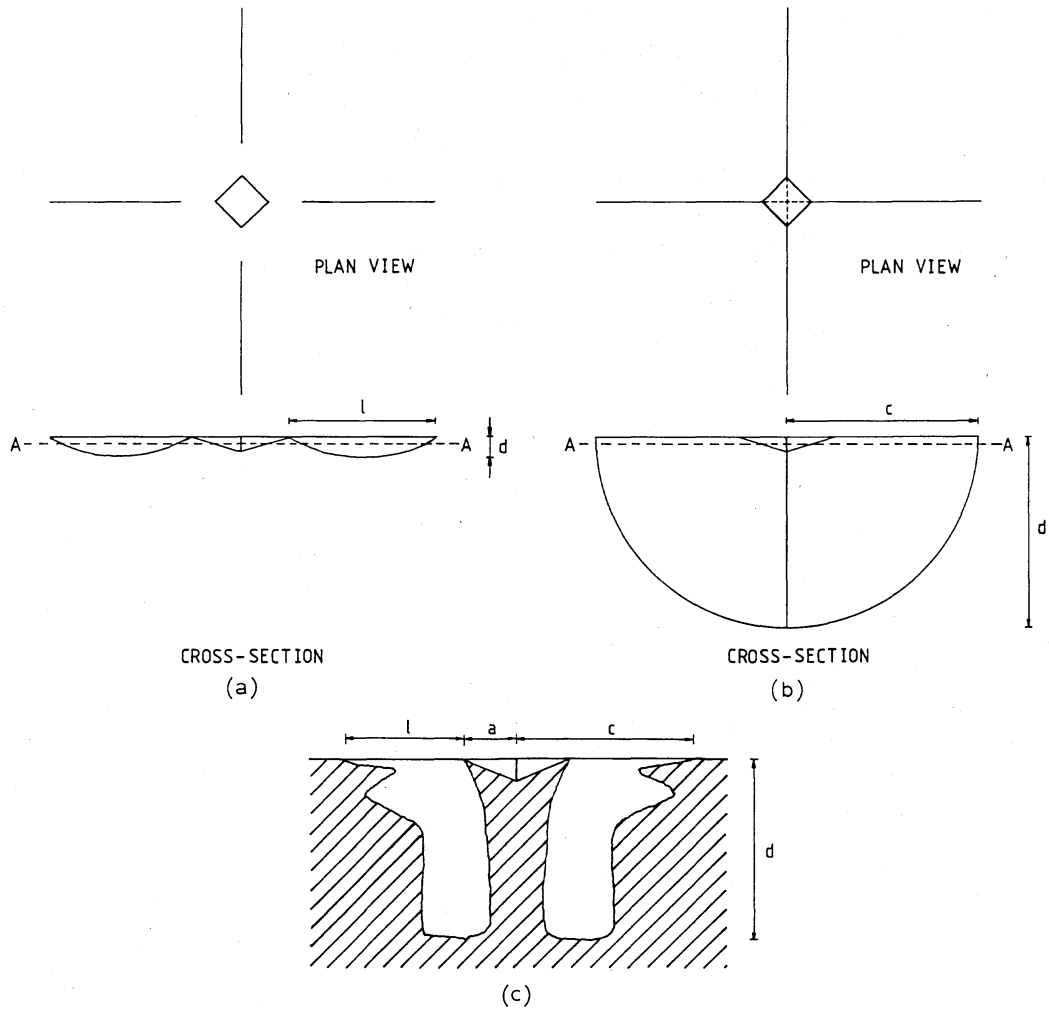

a, b schematic plan view of Vickers crack system after serial polishing of original surface down to plane AA for idealised radial–median (halfpenny) and idealised Palmqvist system, respectively; *c* actual cross-section through surface radial crack plane showing deep Palmqvist cracks formed by Vickers indenter in Silceram SCR19.34

1 Vickers crack systems

order of magnitude as SCR19.34. Serial polishing of the hot press sintered Silceram glass ceramics also revealed the presence of Palmqvist cracks which had penetrated deeper than the indentation depth.

The implication is that all the Silceram glass ceramics develop Palmqvist cracks of the form depicted in Fig. 1*c* when indented at a load of 49 N; however, it cannot be assumed that the Silcerams would also develop such cracks at higher indenter loads nor that all glass ceramics develop such Palmqvist crack profiles. Yet a study by Shetty *et al.*[31] of the Vickers indent crack profiles in Pyroceram 9606 glass ceramic (made from a parent glass in the system $MgO–Al_2O_3–SiO_2$) has shown that Palmqvist cracks, penetrating deeper than the indent itself, develop on indentation at loads in the range 50–200 N. Also, the crack profiles developed at 200 N were similar to those depicted in Fig. 1*c*, except that d/l was ~ 1.

It is well documented that typical WC–Co cermets (having cobalt contents >5 vol.-%) develop Palmqvist cracks as a result of Vickers indentation,[6, 10, 29, 32] with the bulk of the evidence indicating that the cracks extend to a depth greater than that of the indent itself.[6, 29, 32] However, in contrast to SCR19.34 and Pyroceram 9606, the d/l aspect ratio of the Palmqvist cracks in such WC–Co cermets is $\sim 0{\cdot}4$ to $0{\cdot}5$.[6, 29]

Serial polishing of the Vitox alumina, ZTA ceramic, and the TZP ceramics A, B, and C indicated that the TZP and ZTA ceramics had developed Palmqvist cracks that penetrated deeper than the indent depth, while it was found that the Vitox alumina had developed halfpenny cracks. Residual damage zones were evident at the sites of the original indents in the Vitox and ZTA ceramics, but the damage was greater in the Vitox; the absence of residual damage in the TZP ceramics implies that it is a feature characteristic of an alumina matrix. Lateral cracking in the Vitox alumina manifested itself as interference fringes within the quadrants bounded by the surface radial cracks.

These inferred crack profiles are consistent with the data of other workers on the Vickers indentation crack profiles formed in alumina, ZTA, and TZP ceramics. It has been reported that Palmqvist cracks developed in Y_2O_3 TZP at loads of 24–294 N (Ref. 28) and 294 N (Ref. 33) and in CeO_2 TZP at loads of 200–500 N (Ref. 34). However, at much higher indenter loads, halfpenny cracks have been reported to form: at 530 N in Y_2O_3 TZP (Ref. 28) and at $\geqslant 600$ N in CeO_2 TZP (Ref. 34). Calculating the d/l aspect ratio values for the TZP ceramic data of Jones *et al.*[28] and Sullivan and Lauzon[33] gives $d/l = 1{\cdot}1–1{\cdot}6$ with a mean value of $1{\cdot}3 \pm 0{\cdot}2$. Concerning the crack depth d, Jones *et al.*[28] found that the Palmqvist cracks in the TZP were deeper than the indents, which is consistent with the observations of the present authors on TZP and ZTA. Regarding the alumina ceramics, Jones *et al.*[28] have reported that halfpenny cracks developed at loads of 49–530 N, while Sullivan and Lauzon[33] found that halfpenny cracks formed at 294 N. Furthermore, Laugier[35] has reported the forma-

tion of Palmqvist cracks which were deeper than the indentation depths in a ZTA ceramic.

Discussion

The purpose of this paper is to assess the relative merits of the standardised versions of the equations reviewed in Part 1[1] as predictors of the fracture toughness of brittle materials. Thus, for each of the materials to which the equations are applied, there must be a comparative fracture toughness value that is by definition assumed to be the true material fracture toughness. In this paper, the reference fracture toughness is the K_{Ic} toughness as typified by the three point SENB value.

It should be noted that the SENB test gives a fast fracture macrotoughness value K_{Ic} that tends to be an overestimate of the fracture toughness associated with an atomically sharp crack, as a result of the relative bluntness of the notch. By contrast, the Vickers indentation test gives a slow fracture microtoughness value in the sense that crack growth occurs under a constant load applied for a given time which induces an irreversible residual stress that operates both during loading and unloading[1,11] driving the cracks to an equilibrium length. Also, the indentation toughness may be an underestimate of the true material fracture toughness because of the proclivity of many materials to postindentation slow crack growth.

Thus, K_{Ic} and K_c appear to be fundamentally different fracture toughness parameters and hence not comparable. However, it must be remembered that the majority of Vickers indentation fracture toughness equations are calibrated using well documented K_{Ic} data for a range of brittle materials on the basic assumption[1,18] that $K_c \equiv K_{Ic}$. Hence, the Vickers indentation slow fracture microtoughness value, in a sense, will be scaled to give the equivalent fast fracture toughness value. The present authors are therefore of the opinion that $\sigma \equiv K_c/K_{Ic}$ is an acceptable parameter for assessing the relative merits of the standardised indentation equations.

DISCUSSION OF RESULTS FOR EACH CLASS OF MATERIAL

The K_c results given in Tables 2–5 for the individual materials within each class of material, i.e. within the cast Silceram glass ceramics, the hot press sintered Silceram glass ceramics, the aluminas, the zirconia ceramics, and the WC–Co cermets, are considered first. The reader should always bear in mind that (i) the given K_{Ic} value is assumed to be the true material fracture toughness; (ii) only those equations having c/a or l/a range limits satisfied by the experimental data are regarded as giving valid K_c and hence σ values; and (iii) a σ limit of $\sigma = 1{\cdot}00 \pm 0{\cdot}25$, or whatever wider σ limit is necessary to indicate at least the best three equations for a given material, is used as the cut-off point in assessing the relative merits of the valid equations.

Furthermore, the chosen equations are ranked in decreasing order of the closeness of their σ values to $\sigma = 1{\cdot}00$ and identified by their designated letter codes (*see* Table 1 of Part 1[1]); the corresponding σ values are given in the next column. Also, to distinguish them from the standardised versions, whenever K_c data obtained from the *original* versions of the equations are referred to in this paper (Part 2) the *original* equations are identified by their equation number as given in Part 1[1] and printed in bold type.

Table 7 $P/c^{3/2}$ **and** P/l **as function of** P **for Silceram SCF5**

P, N	$P/c^{3/2}$, MN m$^{-3/2}$	P/l, MN m^{-1}
50	18·7	0·369
99	18·8	0·447
149	20·2	0·535

Cast Silceram glass ceramics

The ranked data for these materials are given in Table 6; except for SCR25.76, the same four halfpenny equations, ED, B, NMH1, and JL give the best correlation between K_c and K_{Ic} with σ ranging from 0·92 to 1·09. By contrast, the Palmqvist equation SWMC is best for SCR25.76, with ED, NMH1, JL, and B giving σ values ranging from 0·69 to 0·78.

Comparison of the $P/c^{3/2}$ and P/l values for SCF5 at mean indenter loads P of 50, 99, and 149 N in Table 7 shows that $P/c^{3/2}$ is essentially independent of P, whereas P/l appears to increase with P. Given that all these materials develop Palmqvist cracks and that, except for SCR25.76, halfpenny equations employing the term $(E/H_V)^{2/5}$ appear to give the closest agreement between K_c and K_{Ic}, it is obviously not possible to determine solely from the load dependence of $P/c^{3/2}$ and P/l which crack system develops, i.e. either halfpenny or Palmqvist, nor which theoretical or empirical indentation equation is the most suitable.

Shetty *et al.*[31] came to the same conclusion regarding Corning Pyroceram 9606 glass ceramic and suggested that Palmqvist cracks in ceramics must behave in a manner different from those in WC–Co cermets as a result of the differing aspect ratio d/l of the cracks in the two classes of material. In the Pyroceram 9606, d/l was found to be ~ 1, whereas in typical WC–Co cermets d/l is <1; thus, the Palmqvist cracks in the Pyroceram were apparently behaving as pseudo halfpenny cracks. As d/l was ~ 2 for the Palmqvist cracks in SCR19.34 and assuming, reasonably, that d/l was $\geqslant 1$ in the other cast Silcerams, this explanation would seem to apply to the cast Silcerams, except for SCR25.76. Thus, the behaviour of SCR25.76 cannot be fully explained in terms of the indentation parameters, c/a, l/a,

Table 6 Vickers indentation fracture toughness equations (denoted by letter codes) ranked in order of decreasing closeness of σ to $\sigma = 1{\cdot}00$ for cast Silceram glass ceramics SCF5, SCR19.34, SCR19.13, and SCR25.76

	SCF5		SCR19.34		SCR19.13		SCR25.76	
Rank order	Equation	σ	Equation	σ	Equation	σ	Equation	σ
1	JL	1·00	B	1·02	JL	1·01	SWMC*	1·00
	...	...	...	...	NMH1	1·01	...	...
2	NMH1	0·99	JL	0·97	ED	0·97	B	0·78
3	ED	0·96	NMH1	0·95	B	1·09	JL	0·72
	...	...	...	...	...	...	NMH1	0·72
4	B	1·05	ED	0·92	EC	0·87	ED	0·69
5	MM2	0·86	EC	0·79	MM2	0·85	...	...
6	EC	0·79	MM2	0·76	...	...	...	...

* Palmqvist equation.

Table 8 Vickers indentation fracture toughness equations (denoted by letter codes) ranked in order of decreasing closeness of σ to σ = 1·00 for hot press sintered Silceram glass ceramics SCR19.34 HPC2, HPC3, and HPC4

	SCR19.34 HPC2		SCR19.34 HPC3		SCR19.34 HPC4	
Rank order	Equation	σ	Equation	σ	Equation	σ
1	L3*	0·99	EW	1·01	T	0·97
2	ED	1·05	EC	1·05	EW	1·07
	...	...	...	...	L2	0·93
3	NMH2*	1·06	MM1	0·93	EC	1·11
	EC	0·94	T	0·93	MM1	0·89
	MM1	0·94				
4	B	1·07	L2	0·91	ED	1·12
5	EW	0·89	ED	1·10	ACLM	0·87
	...	...	...	...	L1	0·87
6	SWMC*	1·16	NMH2*	1·12	NMH2*	1·14
	...	...	...	...	B	1·14
7	T	0·83	B	1·13	L3*	1·21
8	L2	0·82	L1	0·86	LEM	0·76
9	NMH1	1·22	ACLM	0·85	...	...
	L1	0·78	...	...	...	...
10	ACLM	0·77	L3*	1·17	...	...
11	...	...	SWMC*	1·25	...	...

* Palmqvist equation.

$P/c^{3/2}$, P/l, and E/H_V, or d/l. However, the microstructure of SCR25.76 could be responsible for its being the only cast Silceram having Palmqvist cracks that appear to be best modelled by a Palmqvist crack model and equation as, unlike the other cast Silceram glass ceramics, its crystal morphology is somewhat euhedral rather than dendritic.[24]

Hot press sintered Silceram SCR19.34 glass ceramics

The ranked results for these materials are given in Table 8; the halfpenny equations EW, EC, ED, B, ACLM, MM1, L1, L2, and T and the Palmqvist equations NMH2 and L3 satisfy $\sigma = 1{\cdot}00 \pm 0{\cdot}25$ for all three materials.

It is instructive to examine those halfpenny equations satisfying, in this particular instance, $\sigma = 1{\cdot}00 \pm 0{\cdot}15$ for cast Silceram SCF5 and SCR19.34 and sintered Silceram SCR19.34 HPC3 and HPC4 as these materials are more than 50 vol.-% crystalline. The satisfactory equations for SCF5 and SCR19.34 employ the term $(E/H_V)^{2/5}$, whereas those for HPC3 and HPC4 employ as a group all the reported exponents of E/H_V, namely, 0, 1/4, 2/5, 1/2, and 2/3. Despite the different exponents of (E/H_V) these nine equations give similar σ values with the result that the mean σ value for HPC3 is $0{\cdot}97 \pm 0{\cdot}10$ (10%), while the mean σ value for HPC4 is $1{\cdot}00 \pm 0{\cdot}11$ (11%).

This implies that when using the HPC2, HPC3, and HPC4 results to calibrate the equation $K_c = k(P/c^{3/2})$,

Table 9 Vickers indentation fracture toughness equations (denoted by letter codes) ranked in order of decreasing closeness of σ to σ = 1·00 for Vitox alumina and alumina of Jones *et al.*[28]

	Vitox		Al_2O_3	
Rank order	Equation	σ	Equation	σ
1	SWMC*	0·93	EC	0·97
2	JL	0·92	T	0·88
3	NMH1	0·89	L2	0·87
4	NMH2*	0·87	L1	0·84
	B	0·87	...	...
5	ED	0·84	ACLM	0·83
6	MM2	0·83	ED	1·25
7	N	1·19	...	...

* Palmqvist equation.

Table 10 $P/c^{3/2}$ and P/l as function of P for alumina of Jones *et al.*[28]

P, N	$P/c^{3/2}$, MN m$^{-3/2}$	P/l, MN m^{-1}
49	32·9	0·532
98·1	34·2	0·629
196	35·3	0·820
294	32·9	0·865
530	41·7	1·26

where k is a constant, averaging the $K_{Ic}/(P/c^{3/2})$ data would give a k value not markedly different from the value of k given by $m(E/H_V)^n$, where m and n are constants obtained by least squares analysis of $\ln[K_{Ic}/(P/c^{3/2})]$ versus $\ln(E/H_V)$. Carrying out such an analysis using the HPC2, HPC3, and HPC4 data gave $m = 0{\cdot}000769$ and $n = 1{\cdot}598$ (correlation coefficient $r = 0{\cdot}9851$); this n value has no theoretical basis (unlike the n values of <1 for the valid halfpenny equations in Table 8; *see* Part 1[1]). Using the E/H_V values in $K_{Ic}/(P/c^{3/2}) = 0{\cdot}000769(E/H_V)^{1{\cdot}598}$ produced a mean predicted $K_{Ic}/(P/c^{3/2})$ value of 0·07798; this compares with the mean experimental $K_{Ic}/(P/c^{3/2})$ value of 0·08005. Thus, for the given set of K_{Ic}, $P/c^{3/2}$, and E/H_V data, both a simple constant factor k and a factor of the form $k = 0{\cdot}000769(E/H_V)^{1{\cdot}598}$ give equally acceptable calibration constants for $K_c = kP/(c^{3/2})$, as previously surmised.

Alumina ceramics

The ranked data for the aluminas are given in Table 9; however, the ZTA data are not included because the toughening behaviour of ZTAs determines that they should be considered with the TZP zirconia ceramics. Only the halfpenny equation ED satisfies $\sigma = 1{\cdot}00 \pm 0{\cdot}25$ for both Vitox and the alumina studied by Jones *et al.*[28], while for each alumina there is only one halfpenny equation that gives a σ value within $0{\cdot}90 < \sigma < 1{\cdot}10$; this is surprising since both aluminas developed halfpenny cracks. Comparing the load dependence of $P/c^{3/2}$ and P/l for the alumina studied by Jones *et al.* over the load range $P = 49$–530 N (*see* Table 10) shows that $P/c^{3/2}$ does not vary with P, while P/l appears to increase with P (as found for Silceram SCF5); this may explain why no Palmqvist equations were suitable.

Rawlings[13] found that the Evans and Charles[36] halfpenny equation **(15)** gave K_c values about 25% lower than the K_{Ic} values for two aluminas having a grain size of ~2 μm. Marion[37] found that the Lawn and Swain[7] and Lawn and Fuller[38] halfpenny equations **(6)** and **(7)**, respectively, gave K_c values about 60% lower than the K_{Ic} values for two aluminas. Anstis *et al.*[18] used the data for two Coors aluminas, AD999 (3 μm grain size, $K_{Ic} = 3{\cdot}9$ MN m$^{-3/2}$) and AD90 (4 μm grain size, $K_{Ic} = 2{\cdot}9$ MN m$^{-3/2}$), when calibrating their halfpenny equation **(24)** and noted without comment that the K_c values lay below the correlation line $K_c \equiv K_{Ic}$. The σ values for AD999 and AD90 are ~0·6 and ~0·7, respectively.

Averaging the σ values for the 14 valid halfpenny equations for Vitox ($K_{Ic} = 6{\cdot}02$ MN m$^{-3/2}$) gives $\sigma = 0{\cdot}65 \pm 0{\cdot}20$ (31%), whereas averaging the σ values for the 13 valid halfpenny equations for the Jones *et al.* alumina ($K_{Ic} = 3$ MN m$^{-3/2}$) gives $\sigma = 1{\cdot}00 \pm 0{\cdot}31$ (31%). For Vitox, all 14 equations produce $\sigma < 1{\cdot}00$, while for the Jones *et al.* alumina eight of the 13 equations produce $\sigma < 1{\cdot}00$; thus, the poor correlation between K_c and K_{Ic} cannot readily be attributed to errors in crack length measurement. This is because the measured crack lengths would tend to err on the short side, which, assuming the calibration constant was derived from reliable and appropriate data, would give K_c values that are too high, i.e. produce σ values >1.

It is possible that the Vitox in particular was subject to postindentation slow crack growth, but while this could account for all the equations giving $\sigma < 1$, it does not explain why a material that forms well developed halfpenny cracks and has a reliable K_{Ic} value[25] is so poorly served by most halfpenny model equations when all the equations would be equally affected by erroneous crack length data resulting from any postindentation slow crack growth. Smith and Pletka[21] have compared the K_c and K_{Ic} data for three alumina ceramics having grain sizes of 2, 9, and 18 μm, designated in this paper as I, II, and III, respectively. They used the Lawn and Fuller[38] and Lawn *et al.*[11] equations **(7)** and **(22)**, respectively, to calculate the K_c data. Their results are summarised in terms of σ values: for equation **(7)** the σ values are 0·40, 0·78, and 0·61 for I, II, and III, respectively, while for equation **(22)** the σ values are 0·41, 1·01, and 0·77 for I, II, and III, respectively. Since it was stated that the measured postindentation slow crack growth data for the three materials were similar, slow crack growth cannot account for the σ values of <1 in view of the good agreement between K_c and K_{Ic} for alumina II, as concluded by Smith and Pletka.

Scatter in the $K_{Ic}/(P/c^{3/2})$ and E/H_V data for alumina may be responsible for the poor agreement between K_c and K_{Ic}. This was investigated by analysing the numerical data extracted from the graphical results of Tanaka[39] for alumina; $K_{Ic}/(P/c^{3/2})$ ranges from 0·0624 to 0·1044 with a mean of $0{\cdot}0867 \pm 0{\cdot}0147$ (17%) while E/H_V ranges from 19·5 to 30 with a mean of $22{\cdot}7 \pm 3{\cdot}7$ (16%). A least squares fit of the $\ln[K_{Ic}/(P/c^{3/2})]$ versus $\ln(E/H_V)$ data gives $m = 0{\cdot}1206$ and $n = -0{\cdot}110$; however, the exponent n in $k = m(E/H_V)^n$ has no theoretical fracture mechanics basis and, owing to the large scatter in the data, $r = -0{\cdot}0992$. Nevertheless, using the equation $K_c = 0{\cdot}1206(E/H_V)^{-0{\cdot}110}(P/c^{3/2})$ gives $\sigma = 0{\cdot}69$ and 1·02 for Vitox and the Jones *et al.* alumina, respectively. These σ values are very close to the corresponding σ values of 0·70 and 1·03 derived from $K_c = 0{\cdot}0867(P/c^{3/2})$; the mean E/H_V value of 22·7 gives k as 0·0855. The above analysis shows that the weak dependence on E/H_V, through n being close to zero or E/H_V not varying much between materials, leads to very similar k values, just as for the sintered Silcerams.

Thus, the poor agreement between K_c and K_{Ic} would not appear to be a result of (i) a proven error in the crack length measurements resulting from slow crack growth; (ii) the value of the exponent of E/H_V; nor (iii) the presumption that the primary assumption of the halfpenny model, namely that halfpenny cracks with $c \gg a$ develop (allowing use of the point force approximation which predicts that $P/c^{3/2}$ is a constant), is satisfied by $c/a = 2{\cdot}6$–$4{\cdot}7$. However, it may be that K_{Ic} data that are not appropriate have been used to calibrate the indentation equations.

Petersson and Bergman[40] carried out a comparison of four fracture toughness test methods applied to Al_2O_3–ZrO_2 ceramics including a pure alumina; the single edge notched beam (SENB), chevron notched beam (CNB), and Vickers indentation strength (VIS) bend tests, and the Vickers indentation toughness (VIT) test were used. They employed the Evans and Davis (as cited in Evans[22]), Lawn *et al.*,[11] and Anstis *et al.*[18] equations **(19)**, **(23)**, and **(26)**, respectively, and found that the measured toughness of the pure alumina decreased in the order VIS > equation **(19)** > SENB > CNB > equation **(26)** > equation **(23)**. Their SENB K_{Ic} value of 4 MN m$^{-3/2}$ and the VIT K_c values were used to calculate the σ values for the VIT equations: the equations rank in decreasing order of the closeness of σ to $\sigma = 1{\cdot}00$ as **(19)**; 1·10 > **(26)**; 0·75 > **(23)**; 0·63. This order is similar to that of the alumina of Jones *et al.* ($K_{Ic} = 3$ MN m$^{-3/2}$), i.e. ED; 1·25 > ACLM; 0·83 > LEM; 0·72.

Lemaitre and Piller[41] measured the fracture toughness of a given alumina using three test methods, i.e. the single edge precracked beam (SEPB), VIS, and VIT techniques; they used the Anstis *et al.*[18] VIT equation **(26)**. It was found that the measured toughness values differed by more than a factor of 2, with toughness decreasing in the order SEPB > VIS > equation **(26)**. This is consistent with the findings of Petersson and Bergman in that the measured SENB and SEPB toughness values are higher than the K_c values obtained from the Anstis *et al.* equation **(26)**; as indeed are the double cantilever beam (DCB) K_{Ic} values of Anstis *et al.*[18] for Coors AD999 and AD90 alumina.

The above data show, for alumina at least, that the notched beam K_{Ic} values are generally higher than the K_c value. The higher K_{Ic} values could result from the notch root radius not being small enough relative to the average grain size, i.e. notch bluntness[42–44] and/or K_{Ic} increasing with crack length, i.e. R curve behaviour.[43,44] During three point SEPB testing under both subcritical displacement controlled and critical load controlled loading, fine grained (~1–3 μm) aluminas display little or no R curve behaviour (as for narrow notch SENB tests[42,43]), whereas coarse grained (~20–40 μm) aluminas exhibit significant R curve behaviour.[45,46] Swain[47] reports that coarse grained (~15–20 μm) alumina displays marked R curve behaviour during DCB K_{Ic} testing, which he suggests should scale with the square of the grain size.

Zirconia and zirconia toughened alumina ceramics

These ceramics employed ZrO_2 stabilised by 3 mol.-%Y_2O_3 enabling the ZrO_2 to be retained in its metastable tetragonal form during cooling from the fabrication temperature; the ZTA contained 20 wt-%ZrO_2. Furthermore, they all developed Palmqvist cracks (under the conditions which produced the K_c data) having mean c/a ratios in the range 1·5–2·3. Thus, the assumption of a residual point force propagating the cracks in the halfpenny model may in some instances be close to its limit of validity.[11,18,48,49]

Table 11 Vickers indentation fracture toughness equations (denoted by letter codes) ranked in order of decreasing closeness of σ to σ = 1·00 for TZP materials A, B, and C; TZP of Jones *et al.*,[28] and ZTA material

	TZP A		TZP B		TZP C		TZP		ZTA	
Rank order	Equation	σ	Equation	σ	Equation	σ	Equation	σ	Equation	σ
1	JL	1·10	L3*	1·03	JL	0·78	EC	0·99	MM1	1·03
2	SWMC*	0·87	JL	0·92	L3*	0·76	NMH2*	0·97	ED	1·06
	...	...	...	...	...	...	...	...	LEM	1·06
3	EC	0·85	SWMC*	0·72	SWMC*	0·65	L3*	1·04	B	1·14
	...	...	...	...	...	...	B	0·96	LF	0·86
4	...	...	...	...	...	...	ED	0·93	EW	1·16
5	...	...	...	...	...	...	EW	0·92	ACLM	1·22
6	...	...	...	...	...	...	SWMC*	1·16	...	...
7	...	...	...	...	...	...	T	0·83	...	...
8	...	...	...	...	...	...	L2	0·79	...	...
9	...	...	...	...	...	...	JL	1·25	...	...

* Palmqvist equation.

Table 12 $P/c^{3/2}$ and P/l as function of P for TZP of Jones *et al.*[28]

P, N	$P/c^{3/2}$, MN m$^{-3/2}$	P/l, MN m^{-1}
24·5	77·0	1·43
49	64·1	1·19
98·1	67·3	1·31
196	60·8	1·47
294	59·4	1·58

The results for these materials are given in Table 11. As always, the possibility that data scatter and/or a fundamental discrepancy between K_c and K_{Ic} may be responsible for the presence or absence of any trends in the σ data, is implicitly acknowledged. Nevertheless, for whatever reason, TZP A, B, and C are better served by the JL halfpenny equation than by the EC halfpenny equation, whereas the opposite is true for the TZP of Jones *et al.* By contrast, both these equations give σ values above 1·30 for the ZTA, with equation JL giving $\sigma = 2{\cdot}06$ (*see* Table 4). Seven halfpenny equations satisfy $\sigma = 1{\cdot}00 \pm 0{\cdot}25$ for ZTA and the TZP of Jones *et al.*, two for TZP A, and one for TZP B and TZP C. Three Palmqvist equations satisfy the σ limit for the TZP of Jones *et al.*, compared to one for TZP A, B, and C, and none for the ZTA. The coefficients of variation for $P/c^{3/2}$ and P/l over the load range 24·5–294 N for the TZP of Jones *et al.* are identical at 11% (*see* Table 5), but if the datum at 24·5 N is excluded, the coefficients are 6 and 12%, respectively. Examination of the $P/c^{3/2}$ and P/l values as a function of indenter load P for $P \geqslant 49$ N suggests that $P/c^{3/2}$ decreases and P/l increases as P increases (*see* Table 12); these apparent variations will be considered further below.

The SENB K_{Ic} and K_c data of Petersson and Bergman[40] for a 22 wt-%ZrO_2 ZTA give a σ ranking (equation numbers are in parentheses) of **(23)**; 1·27 > **(26)**; 1·55 > **(19)**; 2·00 agreeing with LEM > ACLM for the ZTA (*see* Table 11). The TZP data were compared with the K_c data of Matsumoto[34] for a ceria stabilised TZP, the high toughness of which is attributed to ferroelastic domain switching[50] rather than to tetragonal to monoclinic ZrO_2 transformation induced toughening.[51] Of the nine equations he used,[34] eight are reviewed in Part 1[1] and considered here; the ninth equation was $K_c = Z[(H_V a^{1/2})/\phi][E\phi/H_V]^{2/5}$, where Z is determined graphically from the plot of Evans and Charles.[36] The only Matsumoto data used here are his values of K_c derived from data for indenter loads < 500 N, which were used in conjunction with $K_{Ic} = 10{\cdot}2$ MN m$^{-3/2}$ to calculate the corresponding σ values, since under these loads the CeO_2 TZP develops Palmqvist cracks, as do the zirconia ceramics cited in the present paper.

The eight equations used by Matsumoto are: Shetty *et al.*,[6] **(46)**; Lawn *et al.*,[11] **(23)**; Anstis *et al.*,[18] **(26)**; Evans and Davis (*see* Evans[22]), **(19)**; Blendell,[52] **(20)**; Niihara *et al.*,[53] **(27)** and **(29)**; Lankford,[54] **(30)**. Assuming that use of the standardised forms of these equations would not change their rank order, we have LEM > ACLM > ED = B > NMH1 > JL for the halfpenny equations and NMH2 > SWMC for the Palmqvist equations.

WC–Co cermets

The σ data for the Laugier[29] WC–Co cermets are given in Table 13. The Palmqvist equations SWMC, L3, and NMH2 satisfy $\sigma = 1{\cdot}00 \pm 0{\cdot}25$ for WC–5 vol.-%Co, but no Palmqvist equations do so for WC–24 vol.-%Co, even though both cermets developed[29] Palmqvist cracks on indentation at loads between 290 and 490 N. Only the halfpenny equation ED is ranked for both materials, as second and third best equation for WC–5 vol.-%Co and WC–24 vol.-%Co, respectively.

Table 13 Vickers indentation fracture toughness equations (denoted by letter codes) ranked in order of decreasing closeness of σ to $\sigma = 1{\cdot}00$ for WC–Co (vol.-%) cermets of Laugier[29]

	WC–5Co		WC–24Co	
Rank order	Equation	σ	Equation	σ
1	SWMC*	1·03	LF	0·95
2	L3*	0·89	EW	1·16
	ED	1·11	...	...
3	L1	0·85	ED	1·27
4	B	1·16	...	...
	NMH1	1·16	...	...
5	NMH2*	1·17	...	...
6	JL	1·19	...	...
7	ACLM	0·77	...	...
	L2	0·77	...	...

* Palmqvist equation.

The σ data for these cermets will be compared with the results of François and McLaren,[32] who compared the SENB K_{Ic} and Vickers indentation K_c data for WC–5 vol.-%Co and WC–22 vol.-%Co cermets. They used indenter loads of 200–1000 N and the equations of Lawn and Swain,[7] **(6)**; Lawn *et al.*,[11] **(22)**; and Lawn and Fuller,[38] **(7)**. The new standardised versions are LS, LEM, and LF, respectively.

Using their data for the WC–5 vol.-%Co cermet, the σ values ranked the equations in decreasing order of the closeness of σ to 1·00 as **(22)**; 0·67 > **(7)**; 0·56 > **(6)**; 0·36. This order is the same for the Laugier WC–5 vol.-%Co cermet, i.e. LEM; 0·67 > LF; 0·45 > LS; 0·27. For the François and McLaren WC–22 vol.-%Co cermet the equations ranked as **(7)**; 1·12 > **(22)**; 1·36 > **(6)**; 0·36, whereas the order for the Laugier WC–24 vol.-%Co cermet is LF; 0·95 > LS; 0·24 > LEM; 1·59, although the Lawn and Fuller equation gives the σ value nearest to 1·00 for both cermets. This is surprising, since this is a halfpenny equation which assumes that $c/a \geqslant 2$, whereas c/a is $< 1{\cdot}45$ for the WC–24 vol.-%Co cermet.

Shetty and Wright[55] have compared the K_{Ic} and K_c values for WC–Co cermets using the equations of Shetty *et al.*,[6] **(46)** and Anstis *et al.*,[18] **(26)**. They maintain that the Palmqvist model typified by equation **(46)** gives a better correlation between K_{Ic} and K_c than the halfpenny model typified by equation **(26)**. The respective new standardised versions, SWMC and ACLM, give σ values for the WC–Co cermets in the present paper of 1·03 and 0·77 for the Laugier WC–5 vol.-%Co cermet and 1·63 and 1·82 for the Laugier WC–24 vol.-%Co cermet, respectively. These values confirm the findings of Shetty and Wright. Laugier[29] has reported that equation **(26)** increasingly overestimates the fracture toughness of WC–Co cermets as the cobalt content increases. He also claims[56] that indentation models in terms of c/a and l/a are equally valid for WC–Co cermets with $1 \leqslant c/a \leqslant \approx 2$, but by contrast with both Shetty and Wright and the present authors, he found that the Anstis *et al.*[18] model ($P/c^{3/2}$ = constant) gave less scattered results than the Palmqvist model (P/l = constant).

Table 14 $P/c^{3/2}$ and P/l as function of P for WC–Co (vol.-%) cermets of Laugier[29]

P, N	$P/c^{3/2}$, MN m$^{-3/2}$	P/l, MN m^{-1}
WC–5Co		
294	80·2	1·91
392	76·1	1·95
490	72·4	1·97
WC–24Co		
290	214	13·0
392	217	12·3
490	204	9·9

Table 5 indicates that $P/c^{3/2}$ and P/l are independent of P for the WC–5 vol.-%Co cermet, with coefficients of variation of 5 and 3%, respectively, while for the WC–24 vol.-%Co cermet having $c/a < 1{\cdot}5$, the corresponding coefficients are 7 and 23%. However, the data in Table 14 show that as P increases, $P/c^{3/2}$ decreases and P/l increases for the WC–5 vol.-%Co cermet, whereas P/l decreases ($P/c^{3/2}$ may possibly do likewise) for the WC–24 vol.-%Co cermet. The dependence of $P/c^{3/2}$ and P/l on P will be considered in the following section.

Summary of results for each class of material

Those valid equations satisfying $\sigma = 1{\cdot}00 \pm 0{\cdot}10$ for at least half of the materials in a given class of material and $\sigma = 1{\cdot}00 \pm 0{\cdot}35$ for all the materials in the same class, are given below.

1. Cast Silcerams: ED, B, NMH1, JL.
2. Hot press sintered Silcerams: EW, EC, ED, MM1, L2, T.
3. Aluminas: EC, JL.
4. Zirconias
   (i) TZP ceramics: JL
   (ii) ZTA ceramic: no agreement with TZPs or aluminas.
5. WC–Co cermets: ED.

Note that equations JL and ED satisfy the above σ limits for three out of five classes of material.

EFFECT OF SURFACE STRESS STATE ON K_c

The systematic variation of P/l and $P/c^{3/2}$ with P for Silceram SCF5, the alumina and TZP of Jones *et al.*,[28] and the WC–Co cermets of Laugier[29] may be due to residual compressive surface stresses.

The effect of a surface compressive stress (caused by transformation toughening induced by surface grinding) on the indentation toughness of partially stabilised ZrO_2 and HfO_2 ceramics and ZTA ceramics has been studied by Ikuma and Virkar.[57] They used a model after Marshall and Lawn[58] which predicts that the indentation of a compressively stressed surface should lead to a linear plot of positive slope for $(P/c^{3/2})$ versus $c^{1/2}$; since $K_c = kP/(c^{3/2})$, K_c should also be a linear function of $c^{1/2}$. The equation $K_c = Z[(H_V a^{1/2})/\phi][E\phi/H_V]^{2/5}$, where Z is determined graphically from the plot of Evans and Charles,[36] was used to calculate the K_c results. The equations of Blendell,[52] **(20)**, and Evans and Davis (Evans[22]), **(19)**, are likely to give similar K_c values.

The value of K_c was found to increase linearly with increasing $c^{1/2}$ for both ZTA and the partially stabilised ceramics having <6 mol.-% stabilising oxide, but was independent of $c^{1/2}$ for annealed soda–lime glass and (essentially) for alumina. Ikuma and Virkar[57] concluded that a positive dependence of K_c on $c^{1/2}$ together with K_c values that are much higher than the K_{Ic} values are indicative of the presence of induced surface compressive stresses.

Green[59] disputes their conclusions; he studied the K_c versus $c^{1/2}$ behaviour of ZTA ceramics having both stress free and compressively stressed surfaces, using the equations of Evans and Davis (as cited in Evans[22]), **(19)**, and Anstis *et al.*,[18] **(26)**, to calculate the K_c values. Plotting K_c against $c^{1/2}$ for a ZTA having a stress free surface, he found that K_c from equation **(19)** increased linearly as $c^{1/2}$ increased, whereas K_c from equation **(26)** was relatively independent of $c^{1/2}$. It was also found that $P/c^{3/2}$ was independent of $c^{1/2}$ for a stress free surface, but decreased linearly with increasing $c^{1/2}$ for a compressively stressed surface. Green proposed that since c went much deeper than the compressive zone depth ($\sim 40\,\mu m$) in these materials, the value $P/c^{3/2}$ should decrease towards the value for a stress free surface as the indentation load and hence crack length increased (as would K_c when calculated from $K_c = kP/c^{3/2}$, where k is a constant), i.e. as the median cracks grow beyond the compressive stress zone. He thus claimed that the positive variation of K_c with $c^{1/2}$ reported by Ikuma and Virkar is due not to the presence of surface residual stresses, but to the inapplicability of the Evans and Charles[36] indentation fracture model to transformation toughenable ceramics, especially when they have been surface ground.

Ikuma and Virkar[60] refute Green's explanation of their results and, in reply, replotted their PSZ data using the Anstis *et al.* equation,[18] **(26)**, and found that instead of K_c increasing linearly with $c^{1/2}$ as it did when calculated from the plot of Evans and Charles,[36] it decreased linearly. Extrapolation of the PSZ K_c data derived from equation **(26)** to $c^{1/2} = 0$ gave $K_{Ic} = 5\ MN\ m^{-3/2}$, whereas the PSZ data derived using the plot of Evans and Charles produced $K_{Ic} = 3{\cdot}1\ MN\ m^{-3/2}$, which agrees well with the DCB value of $K_{Ic} = 3{\cdot}5\ MN\ m^{-3/2}$ (Ref. 57). They also presented data for two ZTA ceramics designated as ZTA 1 and ZTA 2 in the present paper; ZTA 1 consisted of an inner core, which retained most of its ZrO_2 as tetragonal ZrO_2, and a surrounding outer layer (~ 300 to $> 500\,\mu m$ thick) containing a large fraction of ZrO_2 as monoclinic ZrO_2, i.e. the surface layer was compressively stressed to a depth of $\geqslant 300\,\mu m$. ZTA 2 essentially contained only monoclinic ZrO_2, i.e. its surface was effectively stress free. A plot of the K_c data for both samples (obtained from the Anstis *et al.* equation,[18] **(26)**) against $c^{1/2}$ revealed that K_c showed a sharp linear decrease for ZTA 1, but only a small linear decrease for ZTA 2 as $c^{1/2}$ increased. However, as the deepest crack in ZTA 1 was deemed to be $200\,\mu m$, and therefore wholly contained within the surface compressive stress zone, the Marshall and Lawn[58] model was fully valid and K_c for ZTA 1 would be expected to increase with increasing $c^{1/2}$; this it did if K_c was calculated using the Evans and Charles model.

Thus, Ikuma and Virkar concluded that a decrease in K_c with increasing $c^{1/2}$ does not indicate that the crack is growing beyond the compressive stress zone. Instead, they suggest that this behaviour results from the invalidity at low values of c/a of the point force approximation to the distributed residual crack-driving force in the halfpenny model, $K_c = k(P/c^{3/2})$, since in their work,[57] c/a was often <2, while $c/a > \approx 2$ is the generally accepted lower validity limit for this approximation.

In response to these conflicting explanations as to why the slope of a K_c versus $c^{1/2}$ plot seems to depend on the indentation equation used to calculate the K_c data, Ponton and Rawlings[61] investigated the dependence of K_c on the surface radial crack length as a function of both the Vickers indentation fracture toughness equation used to calculate K_c and the material indented. The $c^{1/2}$ and $l^{1/2}$ data for Silceram SCF5, the alumina and TZP of Jones *et al.*,[28] and the WC–5 vol.-%Co cermet of Laugier[29] were used in conjunction with the K_c data from the standard equations in Part 1[1] to conduct least squares linear regression analyses of the equations $K_c = Ac^{1/2} + B$ and $K_c = Al^{1/2} + B$, where A and B are constants, which are different for each equation and material.

It was concluded that the linear relationship between K_c and $c^{1/2}$ or $l^{1/2}$ is a general one because it (i) appears to hold for both halfpenny and Palmqvist crack systems; (ii) is not a function of E/H_V; and (iii) is not restricted to certain c/a, l/a, or P ranges. However, the results do indicate that the slope of the plot of K_c versus $c^{1/2}$ or $l^{1/2}$ is a function of both the generic form of the indentation equation used and the material, but the slope appears not to depend on c/a or l/a (note $c/a = l/a + 1$). On ignoring the data for equations EW, ED, B, and MM2, and assuming (with good reason) that Silceram SCF5 and alumina do not exhibit the same susceptibility to induced surface compressive stresses as do TZP and WC–Co, some general conclusions regarding the

Table 15 Values of A from $K_c = Ac^{1/2} + B$ that correspond to equations ED, B, and ACLM[1] for Silceram SCF5, alumina and TZP of Jones *et al.*,[28] and WC–5 vol.-%Co cermet of Laugier,[29] and graphically estimated values of A from data of Green[59] and Ikuma and Virkar[60]

Material	Equation		
	ED	B	ACLM
Stress free surface			
SCF5*	0·03	0·05	0·02
Alumina*	0·06	0·09	0·05
TZP*	0·12	0·11	−0·08
WC–5 vol.-%Co*	−0·18	−0·07	−0·19
ZTA (Ref. 59)	~ 0·16	...	~ 0·003
ZTA 2 (Ref. 60)†	...	...	~ −0·05
Compressive surface stress			
PSZ (Ref. 60)‡	~ 0·29	~ 0·29	~ −0·12
ZTA (Ref. 59)§	...	...	~ −0·37
ZTA 1 (Ref. 60)§	~ 0·20	~ 0·20	~ −0·36

* These materials are assumed to be stress free given that they had been diamond polished down to $\leqslant 1$ μm.
† These materials were annealed and/or polished[59] or essentially contained only ZrO_2 in its monoclinic form;[60] thus, they were presumed to be stress free.
‡ Ikuma and Virkar[57,60] were of the opinion that this PSZ ceramic had a surface compressive zone.
§ These materials had a partially transformed surface layer (monoclinic/tetragonal ZrO_2); thus, they possessed a surface compressive stress zone.

sign of the slope can be drawn. The data show that equations of the generic form

$$K_c = kP/(ax^{1/2}) \equiv k(P/a^{3/2})(a/x)^{1/2} \equiv k(P/x)^{1/2}$$

where $x = c$ or l, give K_c values that increase with increasing $x^{1/2}$ for both classes of material, whereas equations of the generic form $K_c = kP/c^{3/2}$ give K_c values that increase with increasing $x^{1/2}$ for materials not susceptible to induced surface compressive stresses and K_c values that decrease with increasing $x^{1/2}$ for materials prone to induced surface compressive stresses.

Ponton and Rawlings[61] estimated the slopes of the graphical plots of K_c and $P/c^{3/2}$ versus $c^{1/2}$ given by Ikuma and Virkar[57,60] and Green[59]; for the ZTA ceramics studied by Green, the $P/c^{3/2}$ values were converted to the equivalent K_c values using equation **(26)**, assuming $E/H_V = 20$. The estimates were compared with the slopes obtained from $K_c = Ac^{1/2} + B$ for the equivalent standardised equations for Silceram SCF5, the alumina and TZP of Jones *et al.*,[28] and the WC–5 vol.-%Co cermet of Laugier.[29] The results are given in Table 15.

Excluding consideration of the WC–Co A values, because of the lack of any data for surface stressed WC–Co cermets, and allowing for the experimental scatter in (i) Fig. 1 of Green[59] for the equation ED data and (ii) in Fig. 1 of Ikuma and Virkar[60] for their PSZ data, the tabulated data tentatively suggest that:

(i) for equations ED and B (although a direct comparison with the corresponding graphical plot of Evans and Charles[36] is not actually possible) a positive A value of the order of $\geqslant 0{\cdot}2$ implies the presence of a surface compressive stress zone
(ii) for equation ACLM, a negative A value of the order of $\geqslant 0{\cdot}1$ indicates the existence of a surface compressive stress zone.

Furthermore, the surface stress model of Marshall and Lawn[58] based on $K_c = kP/c^{3/2}$ as applied to annealed and tempered soda–lime glass appears to be consistent with the trends in Table 15. Using equation LF, which is of the form $K_c = kP/c^{3/2}$, gives $A = 0$ for the annealed soda–lime glass and $A \approx 0{\cdot}1$ for the tempered soda–lime glass. Since the A values from equation LF for Silceram SCF5 and the alumina of Jones *et al.* (which were presumed to have stress free surfaces) are 0·01 and 0·03, respectively,[61] it might be expected that K_c as calculated from $K_c = kP/c^{3/2}$ for low toughness materials (i.e. $K_{Ic} < 4$ MN m$^{-3/2}$) would increase markedly with increasing $c^{1/2}$ if the test surfaces were compressively stressed. Finally, it is recommended that a strong linear dependence of K_c on $c^{1/2}$ should not be considered indicative of a surface compressive stress unless K_c versus $c^{1/2}$ data for the stress free surface condition are also available for comparison.

DISCUSSION OF PERFORMANCE OF EQUATIONS

Ability of equations to correlate K_c and K_{Ic}

Having already discussed above the K_c and σ data for the materials within each class of material, attention is now given to the correlation between K_c and K_{Ic} produced by each of the valid indentation equations for all 16 materials. The σ values in Tables 6, 8, 9, 11, and 13 were used to determine the best three equations for each of the 16 materials. The total number of first, second, and third rank placings of each valid equation, denoted by Σ1st, Σ2nd, and Σ3rd, respectively, was then determined, together with the sum of first and second placings and the sum of first, second, and third placings, denoted by Σ(Σ1st + Σ2nd) and Σ(Σ1st + Σ2nd + Σ3rd), respectively. The equations are thus ranked in Table 16 on the premise that the order of decreasing precedence is Σ1st > Σ2nd > Σ(Σ1st + Σ2nd) > Σ3rd > Σ(Σ1st + Σ2nd + Σ3rd). Using the sum of

Table 16 Frequency of satisfactory performance by indentation equations in terms of three σ values which are nearest to σ = 1·00 for each material as evaluated from σ data for all sixteen materials

Equation[1]	Σ1st	Σ2nd	Σ(Σ1st + Σ2nd)	Σ3rd	Σ(Σ1st + Σ2nd + Σ3rd)	SC
JL	4	3	7	1	8	15
SWMC*	3	1	4	2	6	10
L3*	2	2	4	1	5	9
EC	2	1	3	3	6	9
EW	1	2	3	0	3	6
B	1	1	2	3	5	7
NMH1	1	1	2	3	5	7
T	1	1	2	1	3	5
MM1	1	0	1	3	4	5
LF	1	0	1	1	2	3
ED	0	4	4	2	6	10
LEM	0	1	1	0	1	2
L2	0	1	1	1	2	3
NMH2*	0	1	0	1	2	2
L1	0	0	0	1	1	1

* Palmqvist equation.
SC = Σ(Σ1st + Σ2nd) + Σ(Σ1st + Σ2nd + Σ3rd), which is used as the equation selection criterion; the greater the SC the better the correlating ability of a given equation.

$\Sigma(\Sigma 1st+\Sigma 2nd)$ and $\Sigma(\Sigma 1st+\Sigma 2nd+\Sigma 3rd)$, which gives greater weighting to $\Sigma(\Sigma 1st+\Sigma 2nd)$, as the selection criterion for correlating ability, it can be seen that equation JL gives the best result, in agreement with the data given above in 'Summary of results for each class of material'; equations SWMC and ED are second, while equations L3 and EC are third.

In an attempt to evaluate the overall correlating ability of each equation as regards the five material classes, all the valid σ values (i.e. the valid K_c values by inference) from each equation were averaged. The mean σ value σ_m, the sample standard deviation σ_s, the coefficient of variation σ_v and the number of σ values averaged N corresponding to each equation are given in Table 17. Using the decreasing precedence order $(N \geqslant 12) > (\sigma_m = 1{\cdot}00 \pm 0{\cdot}25) > (\sigma_v \leqslant 30\%)$ as the selection criterion, equations B, ED, EC, and SWMC may be considered to be the most satisfactory.

The above two selection criteria, employing the data in Tables 16 and 17, appear to show that equations ED, EC, and SWMC may be the best all-round equations to use if one wants to, or must, determine the fracture toughness of a ceramic material using the Vickers indentation test rather than one of the conventional fracture toughness tests, e.g. the SENB test. However, the data in Tables 16 and 17 give no information regarding the relative abilities of the equations to rank materials in the order of the fracture toughness measured conventionally; this performance aspect of the equations will be considered in the following section.

Ability of equations to rank materials according to their fracture toughness

The preceding discussions of the results have concentrated on the ability of the Vickers indentation equations to give K_c values close to K_{Ic} for the individual materials as measured by σ, i.e. K_c/K_{Ic}. The actual K_c and K_{Ic} data in Tables 2–5 are now considered. Table 2 shows that all the valid equations rank the toughness of three of the cast Silceram glass ceramics, SCF5, SCR19.34, and SCR19.13, in the same order as the SENB K_{Ic} toughness, namely, SCF5 > SCR19.34 > SCR19.13, even though equation EW, not being valid for SCR19.13 because $c/a > 4{\cdot}5$, gives a negative K_c value for SCR19.13. However, SCR25.76, which is the toughest Silceram according to the K_{Ic} data, appears to be incorrectly ranked by all the valid equations which give SCF5 > SCR19.34 $\geqslant$ SCR25.76 > SCR19.13. This could be because of a difference in the SENB notch and indentation crack propagation behaviour of SCR25.76 resulting from its crystal morphology, which being different from that of the other cast Silcerams, may also be responsible for the SWMC Palmqvist equation being the only one to satisfy $\sigma = 1{\cdot}00 \pm 0{\cdot}25$ for SCR25.76, giving as it does $\sigma = 1{\cdot}00$.

Considering the three hot press sintered Silceram SCR19.34 glass ceramics and the Vitox alumina, Table 3 shows that all the valid equations, excluding MM1 (which is in fact not valid for Vitox), rank the materials in the same order of toughness as the SENB K_{Ic} values; Vitox alumina > SCR19.34 HPC4 > SCR19.34 HPC3 > SCR19.34 HPC2. Equation MM1 ranks the sintered Silcerams as SCR19.34 HPC3 $\approx$ SCR19.34 HPC4 $\approx$ SCR19.34 HPC2, but the differences in K_c are too small to give a definite toughness ranking; equation LS also ranks SCR19.34 HPC3 $\approx$ SCR19.34 HPC4. Regarding the relative toughness of the Vitox and the Jones *et al.* alumina ceramics (*see* Tables 3 and 5), the K_{Ic} values rank them as Vitox > Jones *et al.* alumina, as do all the valid equations, except equation LS which ranks them in reverse order. Also in Table 5, the two WC–Co cermets are ranked in the same order of toughness by both the K_{Ic} and K_c values.

So far, the agreement between the K_{Ic} and K_c fracture toughness rankings has been acceptable; however, according to Tables 4 and 5, the K_{Ic} and K_c toughness rankings for the TZP and ZTA ceramics exhibit different trends. The K_{Ic} data ranks these materials by toughness as TZP B > TZP C > TZP A > ZTA > TZP (Jones *et al.*), but all the valid equations, except LS and MM1, rank them as ZTA > TZP A > TZP B > TZP C > TZP. Equation LS gives ZTA > TZP A > TZP B > TZP > TZP C, while equation MM1 gives ZTA > TZP A = TZP B > TZP C > TZP. Thus, the only agreement between the K_{Ic} and K_c data (including the LS and MM1 results) as regards the ranking is: (i) ZTA > TZP; (ii) TZP B > TZP C; and (iii) TZP A, TZP B > TZP.

However, if the LS and MM1 results are excluded, (iii) becomes TZP A, TZP B, TZP C > TZP. Furthermore, ignoring the LS ranking gives the K_c ranking TZP B > TZP C > TZP, in agreement with the K_{Ic} ranking. Thus, equation LS has the worst ranking ability in terms of K_c, which is in keeping with its giving, on balance, the worst σ values for these materials.

Fracture toughness correlating and ranking ability of Vickers indentation technique

To assess the ability of the Vickers indentation technique both to correlate and rank the indentation toughness relative to the toughness obtained by other means, all the valid K_c values for each material were averaged and the corresponding σ value calculated. The results are given in Table 18, together with the sample standard deviation and coefficient of variation for the mean K_c values, as well as the number of K_c values averaged, and the K_{Ic} value. The average σ value was $0{\cdot}89 \pm 0{\cdot}33$ (37%); if the very high σ value for WC–24 vol.-%Co is excluded, the mean σ value is $0{\cdot}83 \pm 0{\cdot}21$ (25%). Thus, the overall correlating ability is reasonably good, i.e. within 20% on average. Concerning the ranking ability, the K_{Ic} and K_c rankings are in agree-

Table 17 Mean σ value σ_m, sample standard deviation σ_s, and coefficient of variation σ_v for each indentation equation as obtained by averaging all valid σ values produced by given equation ($\sigma \equiv K_c/K_{Ic}$), together with number of σ values averaged N (σ data are given in Tables 2–5)

Equation	σ parameters			
	σ_m	σ_s	σ_v, %	N
Group A				
B	0·99	0·27	27	16
ED	0·93	0·25	27	16
EC	0·91	0·26	29	16
SWMC*	1·21	0·35	29	16
Group B				
T	0·82	0·29	35	16
EW	0·76	0·27	36	14
L2	0·81	0·33	41	16
ACLM	0·77	0·34	44	16
L1	0·79	0·41	52	16
Group C				
JL	1·27	0·55	43	16
L3*	1·28	1·38	108	16
LEM	0·67	0·30	45	16
LF	0·57	0·16	28	16
LS	0·29	0·11	38	16
Group D				
NMH2*	1·05	0·40	38	11
MM1	0·82	0·43	52	9
NMH1	1·03	0·19	18	8
MM2	0·97	0·34	35	7
N*	1·45	0·16	11	6

* Palmqvist equation.
Group A satisfies $N \geqslant 12$, $\sigma_m = 1{\cdot}00 \pm 0{\cdot}25$ and $\sigma_v \leqslant 30\%$.
Group B does not satisfy $\sigma_v \leqslant 30\%$.
Group C does not satisfy $\sigma_m = 1{\cdot}00 \pm 0{\cdot}25$.
Group D does not satisfy $N \geqslant 12$.

Table 18 Mean K_c value of N valid K_c values for each of 16 materials, together with corresponding K_{Ic} and σ ($\equiv K_c/K_{Ic}$) values (σ, K_c, K_{Ic} data are given in Tables 2–5)

Material	K_c, MN m$^{-3/2}$	N	K_{Ic}, MN m$^{-3/2}$	σ
SCF5	1·51 ± 0·52 (34%)	16	2·02	0·75
SCR19.34	1·32 ± 0·46 (35%)	16	1·83	0·72
SCR19.13	0·87 ± 0·37 (43%)	15	1·06	0·82
SCR25.76	1·24 ± 0·45 (36%)	16	2·29	0·54
SCR19.34 HPC2	2·20 ± 0·64 (29%)	18	2·36	0·93
SCR19.34 HPC3	2·42 ± 0·70 (29%)	17	2·42	1·00
SCR19.34 HPC4	2·57 ± 0·74 (29%)	17	2·51	1·02
Vitox	4·25 ± 1·38 (32%)	18	6·02	0·71
Al_2O_3	3·09 ± 1·11 (36%)	15	3	1·03
TZP	4·80 ± 1·42 (30%)	17	5·5	0·87
TZP A	6·61 ± 2·52 (38%)	16	9·43	0·70
TZP B	6·24 ± 2·21 (35%)	16	10·76	0·58
TZP C	5·42 ± 1·69 (31%)	16	10·73	0·51
ZTA	8·31 ± 3·38 (41%)	16	6·5	1·28
WC–5 vol.-%Co	8·12 ± 3·03 (37%)	18	8·8	0·92
WC–24 vol.-%Co	21·39 ± 14·39 (67%)	16	11·5	1·86

ment for the alumina and TZP of Jones *et al.*, the WC–Co cermets of Laugier, the hot press sintered Silceram SCR19.34 glass ceramics, and the cast Silceram glass ceramics SCF5, SCR19.34, and SCR19.13.

The apparent disagreement between the K_c and K_{Ic} rankings for the remaining materials is considered below. Possible reasons as to why the Silceram SCR25.76 results are anomalous (as regards either the K_c or K_{Ic} values) have been put forward already. Concerning the generally poor correlation between the K_c values from halfpenny equations and the K_{Ic} values for alumina, it is possible that the use of inappropriate calibration data and/or a basic difference in the indentation crack and notch crack propagation behaviour of alumina may be responsible. The effect of R curve behaviour during K_{Ic} tests is only significant for coarse grained aluminas (*see* 'Alumina ceramics' above). As far as the fine grained Vitox alumina is concerned, the low average σ value of 0·71 for the 18 valid equations and 0·65 for the 14 valid halfpenny equations may result from its average grain size of 3 μm affecting the indentation crack propagation, as might be inferred from the data presented below.

1. Rawlings[13] found that equation **(15)** produced a σ value of ~0·75 for two aluminas with a mean grain size of ~2 μm.

2. The present authors used the graphical K_c and numerical K_{Ic} data of Anstis *et al.*[18] for Coors AD999 and AD90 aluminas to estimate their respective σ values; it was found that σ was ~0·6 for AD999 of 3 μm grain size and ~0·7 for AD90 of 4 μm grain size.

3. Smith and Pletka[21] reported data for three alumina ceramics, designated as I, II, and III in this paper, having grain sizes of 2, 9, and 18 μm, respectively. Using their K_c and K_{Ic} data, the respective average σ values are 0·41, 0·90, and 0·69.

These results would seem to suggest that a grain size of the order of 2–3 μm may in some way correspond to a poor correlation between K_c and K_{Ic}; however, it may just be a coincidence. For example, Petersson and Bergman[40] have reported toughness data for an alumina having an alumina matrix grain size of 1·6 μm, containing a 0·52 volume fraction of 7 × 3 μm tabular alumina grains and 1·5% porosity. The fracture toughness data were obtained using the halfpenny indentation equations **(19)**, **(23)**, and **(26)**, and the SENB, CNB, and VIS bending tests (*see* 'Alumina ceramics'); the present authors used the SENB K_{Ic} value to calculate a mean σ value of 0·83 ± 0·24 (29%). Also, since no grain size data were available for the alumina of Jones *et al.*,[28] the average σ value of 1·03 for all 15 valid equations and 1·00 for all 13 valid halfpenny equations cannot be commented upon.

The TZPs A, B, and C have mean σ values of $\leqslant$0·7; however, both crack length measurement errors, which tend to err on the short side, and pre-existing compressive surface stresses would be expected to give $\sigma > 1$. Another possible explanation could be that the SENB K_{Ic} values were overestimated because of a notch width sensitivity and/or K_{Ic} increasing with increasing relative notch depth, i.e. R curve behaviour; a notch width of 0·15 mm and relative depth* range of 0·2–0·4 were used as for the ZTA ceramic.

Concerning the ZTA results, Petersson and Bergman[40] found that the K_c values (calculated using equations **(19)**, **(23)**, and **(26)**) for a 22 wt.-%ZrO_2 ZTA were higher than the toughness determined using the SENB, CNB, and VIS methods (*see* 'Alumina ceramics'). They suggest that the lower K_{Ic} values of the high zirconia content (e.g. ~20 wt.-%ZrO_2) ZTA materials, are the result of microcracks (formed on cooling from the sintering temperature as tetragonal ZrO_2 transforms to monoclinic ZrO_2) linking up during loading in the SENB, CNB, and VIS bending beam toughness tests, thus leading to a low K_{Ic} value. By contrast, the Vickers indentation test, being a localised microfracture test and thus sampling a smaller material volume, is not likely to cause the inherent microcracks to join up sufficiently to produce a decrease in toughness.

Last, having found from Table 18 that the K_c and K_{Ic} rankings are in agreement for 10 of the 16 materials, the combined correlating and ranking ability of the equations as regards these 10 materials can now be assessed. According to Table 17, equations EC, ED, B, and SWMC display the best all-round correlating ability for all 16 materials; hence, the σ values produced by each of these four equations for the Jones *et al.* TZP and alumina, the Laugier WC–Co cermets, the hot press sintered Silceram SCR19.34 glass ceramics HPC2, HPC3, and HPC4, and the cast Silceram glass ceramics SCF5, SCR19.34, and SCR19.13 were averaged. The results are:

$$\sigma(\text{EC}) = 0{\cdot}97 \pm 0{\cdot}23\ (24\%)$$
$$\sigma(\text{ED}) = 1{\cdot}07 \pm 0{\cdot}13\ (12\%)$$
$$\sigma(\text{B}) = 1{\cdot}14 \pm 0{\cdot}15\ (13\%)$$
$$\sigma(\text{SWMC}) = 1{\cdot}37 \pm 0{\cdot}28\ (20\%)$$

Thus, equations ED, EC, and B appear to possess the best combined correlating and ranking abilities as far as these 10 materials are concerned. Finally, although the σ values produced by EW for the alumina and Silceram SCR19.13 were invalid and therefore not used, the mean σ value was 0·83 ± 0·26 (31%).

Conclusions

From the detailed discussion in this paper and Part 1,[1] the following generalised conclusions have been drawn regarding the Vickers indentation fracture toughness test and the various K_c equations.

1. The test sample surface should be stress free before indentation and hence should be carefully polished down to at least 1 μm to remove any prior surface damage; also when the material is susceptible to induced surface residual compressive stresses, e.g. cermets and transformation toughenable ceramics, annealing after polishing, but before indentation, may be necessary.

2. A minimum indenter load of ~50 N is recommended if the surface radial crack lengths are to be measured optically, as this will give acceptable accuracy relative to obtaining the measurements using SEM.

*Relative depth ≡ notch depth/specimen thickness parallel to notch depth.

3. To ensure that the crack length measurement errors are kept to a minimum, the largest indenter load that does not cause lateral crack breakthrough at the surface should be used. In addition, the resultant c/a values will be large enough to avoid elastic–plastic stress field interaction effects near the indent corners which would (i) affect the propagation of the cracks into the elastic matrix surrounding the indentation plastic deformation zone and (ii) invalidate the assumption of the point force indentation model that $c \gg a$; in practice $c/a > \approx 2$.

4. The test sample should be about $20c$ in thickness and have little or no porosity, while adjacent indent centres should be no closer than about $4c$.

5. To minimise the effect of postindentation slow crack growth, the indentation crack lengths should be measured as soon as is practicable after indentation.

6. It is preferable to coat the polished specimen test surface with gold before indentation as this will reduce the time between indentation and crack length measurement; also precoating will not affect the postindentation crack length, whereas postcoating may do so.

7. Dye penetrants should be used with caution, as they may enhance postindentation slow crack growth; if they are used and slow crack growth is observed, the effect on the apparent surface radial crack length must be taken into account when calculating the fracture toughness.

8. For consistency and comparability between the K_c toughness values obtained using the various equations, it is suggested that the standardised versions (of the original equations) given by the authors in Part 1[1] are used.

9. There is no consistent relationship between the performance of a given equation, be it a halfpenny or Palmqvist model equation, and the subsurface crack propagation behaviour of ceramics, i.e., whether halfpenny or Palmqvist cracks are actually developed. For most intents and purposes, halfpenny and Palmqvist equations give equally valid data regardless of the crack profile developed in any given material.

10. The existence of a positive or negative linear dependence of K_c on $c^{1/2}$ over a reasonably wide indenter load range, e.g. 50–150 N, should not be accepted as evidence for the presence of a compressively stressed surface layer in the absence of K_c versus $c^{1/2}$ data for the truly stress free surface condition.

11. If, because the materials or the available samples are not amenable to any of the conventional fracture toughness tests, the Vickers indentation toughness test has to be used to measure the inherent fracture toughness of the materials within a given material class, it is recommended that equations JL and ED are used (*see* 'Summary of results for each class of material'), while for materials not in the same class, equations B, ED, EC, and SWMC should be used (*see* 'Ability of equations to correlate K_c and K_{Ic}, and Tables 16 and 17).

12. Any of the standardised equations in Part 1,[1] except equation LS, can be used qualitatively to rank materials within a given class, provided the c/a or l/a criterion of any chosen equation is satisfied by the material data. That is, essentially identical materials can be ranked via K_c in the same order as they would be in terms of their K_{Ic} values, e.g. the cast Silcerams SCF5, SCR19.34, SCR19.13; the hot press sintered SCR19.34 Silcerams; the two alumina ceramics; the WC–Co cermets. The TZPs A, B, and C and ZTA ceramics, which are identical in the sense that they are all ZrO_2 transformation toughened ceramics, are an exception; however, factors such as the surface stress state of the test sample, the microstructure, and the operative transformation induced toughening mechanisms, etc., may have affected their indentation cracking behaviour, resulting in the different K_c and K_{Ic} toughness rankings.

13. When attempting to rank different materials via K_c, anomalous behaviour is sometimes observed in that certain materials are misranked by K_c relative to the K_{Ic} ranking. There is a number of possible reasons for this, such as microstructural features, e.g. Vitox alumina and the Silceram glass ceramic SCR25.76, and transformation toughening as well as possible R curve behaviour in ZTAs and TZPs. None the less, the average K_c from the valid equations for each material is capable of qualitatively ranking the TZP and alumina of Jones *et al.*, the WC–Co cermets of Laugier, the hot press sintered Silceram SCR19.34 glass ceramics HPC2, HPC3, and HPC4, and the cast Silceram glass ceramics SCF5, SCR19.34, and SCR19.13 in the same order of toughness as K_{Ic} typified by the SENB K_{Ic} values (*see* 'Ability of equations to rank materials according to their fracture toughness' and Table 18). Therefore, any equation (which can be validly used) would probably be able to rank qualitatively more materials in order of toughness via K_c than it could characterise in terms of a K_c/K_{Ic} ratio of ~ 1.

14. As regards the quantitative ranking of different materials in order of toughness, i.e. combining both correlating and ranking ability, it is suggested that equations EC, ED, and B are used (*see* 'Ability of equations to rank materials according to their fracture toughness'), because they are capable of ranking the TZP and alumina of Jones *et al.*, the WC–5 vol.-%Co and WC–24 vol.-%Co cermets of Laugier, the hot press sintered Silceram SCR19.34 glass ceramics HPC2, HPC3, and HPC4, and the cast Silceram glass ceramics SCF5, SCR19.34, and SCR19.13 in the same order of toughness as K_{Ic} while at the same time correlating K_c and K_{Ic} such that the mean of all 30 σ values is $1{\cdot}06 \pm 0{\cdot}18$ (17%).

15. As a generalisation (to which there are always exceptions) it appears that the majority of the 19 Vickers indentation toughness equations may be capable of producing a correlation between K_c and K_{Ic} of 0·8 : 1 to an experimental accuracy of the order of 30%.

In summary, the Vickers indentation fracture toughness test technique has experimental advantages which, on balance, outweigh the disadvantages, particularly when it is used in a brittle materials development programme to (i) rank the materials in terms of fracture toughness and (ii) to measure the intrinsic fracture toughness of those materials for which conventional toughness test methods are not suitable for whatever reason.

Acknowledgments

The authors thank the SERC for financial support and Professor D. W. Pashley, FRS for the provision of research facilities. They also thank M. Cox, D. Evans, H. S. Kim and Dr I. Thompson for their help in obtaining the toughness data for TZPs A, B, and C, the ZTA, and the Silcerams.

References

1. C. B. PONTON and R. D. RAWLINGS: *Mater. Sci. Technol.*, 1989, **5**, (9),. 865–872.
2. D. B. MARSHALL, A. G. EVANS, B. T. KHURI YAKUB, J. W. TIEN, and G. S. KINO: *Proc. R. Soc.*, 1983, **A385**, 461–475.
3. F. F. LANGE, M. R. JAMES, and D. J. GREEN: *J. Am. Ceram. Soc.*, 1983, **66**, (2), C16–C17.
4. R. F. COOK, B. R. LAWN, T. P. DABBS, and P. CHANTIKUL: *J. Am. Ceram. Soc.*, 1981, **64**, (9), C121–C122.
5. D. J. GREEN, F. F. LANGE, and M. R. JAMES: *J. Am. Ceram. Soc.*, 1983, **66**, (9), 623–629.
6. D. K. SHETTY, I. G. WRIGHT, P. N. MINCER, and A. H. CLAUER: *J. Mater. Sci.*, 1985, **20**, 1873–1882.
7. B. R. LAWN and M. V. SWAIN: *J. Mater. Sci.*, 1975, **10**, 113–122.

8. A. G. EVANS and T. R. WILSHAW: *Acta. Metall.*, 1976, **24**, 939–956.
9. B. R. LAWN, M. V. SWAIN, and K. PHILLIPS: *J. Mater. Sci.*, 1975, **10**, 1236–1239.
10. I. M. OGILVY, C. M. PERROTT, and J. W. SUITER: *Wear*, 1977, **43**, 239–252.
11. B. R. LAWN, A. G. EVANS, and D. B. MARSHALL: *J. Am. Ceram. Soc.*, 1980, **63**, (9–10), 574–581.
12. D. B. MARSHALL, B. R. LAWN, and A. G. EVANS: *J. Am. Ceram. Soc.*, 1982, **65**, (11), 561–566.
13. R. D. RAWLINGS: *Mater. Sci. Eng.*, 1983, **61**, L1–L5.
14. A. G. EVANS, M. E. GULDEN, and M. ROSENBLATT: *Proc. R. Soc.*, 1978, **A361**, 343–365.
15. B. R. LAWN, D. B. MARSHALL, and P. CHANTIKUL: *J. Mater. Sci.*, 1981, **16**, 1769–1775.
16. R. F. COOK and D. H. ROACH: *J. Mater. Res.*, 1986, **1**, (4), 589–600.
17. B. R. LAWN and T. R. WILSHAW: *J. Mater. Sci.*, 1975, **10**, 1049–1081.
18. G. R. ANSTIS, P. CHANTIKUL, B. R. LAWN, and D. B. MARSHALL: *J. Am. Ceram. Soc.*, 1981, **64**, (9), 533–538.
19. P. K. GUPTA and N. J. JUBB: *J. Am. Ceram. Soc.*, 1981, **64**, (8), C112–C114.
20. D. B. MARSHALL and B. R. LAWN: *J. Mater. Sci.*, 1979, **14**, 2001–2012.
21. S. S. SMITH and B. J. PLETKA: in 'Fracture mechanics of ceramics', Vol. 6, 'Measurements, transformations and high temperature fracture', (ed. R. C. Bradt *et al.*), 189–209; 1983, New York, Plenum Press.
22. A. G. EVANS: in 'Fracture mechanics applied to brittle materials', STP 678, (ed. S. W. Freiman), 112–135; 1979, Philadelphia, PA, ASTM.
23. J. J. PETROVIC: *J. Am. Ceram. Soc.*, 1983, **66**, (4), 277–283.
24. S. CARTER, C. B. PONTON, R. D. RAWLINGS, and P. S. ROGERS: *J. Mater. Sci.*, 1988, **23**, 2622–2630.
25. M. W. REAL, D. R. COOPER, R. MORRELL, R. D. RAWLINGS, B. WEIGHTMAN, and R. W. DAVIDGE: *J. Phys. (Orsay)*, 1986, **47**, (2), Colloque C1, 763–767.
26. H. S. KIM: PhD thesis, Dept of Materials, Imperial College, 1989.
27. D. B. MARSHALL, TATSUO NOMA, and A. G. EVANS: *J. Am. Ceram. Soc.*, 1982, **65**, (10), C175–C176.
28. S. L. JONES, C. J. NORMAN, and R. SHAHANI: *J. Mater. Sci. Lett.*, 1987, **6**, 721–723.
29. M. T. LAUGIER: *J. Mater. Sci. Lett.*, 1987, **6**, 897–900.
30. J. L. CHERMANT and F. OSTERSTOCK: *J. Mater. Sci.*, 1976, **11**, 1939–1951.
31. D. K. SHETTY, A. R. ROSENFIELD, and W. H. DUCKWORTH: *J. Am. Ceram. Soc.*, 1985, **68**, (10), C282–C284.
32. J.-P. FRANÇOIS and J. R. McLAREN: *Proc. Br. Ceram. Soc.*, 1982, **32**, 227–235.
33. J. D. SULLIVAN and P. H. LAUZON: *J. Mater. Sci. Lett.*, 1986, **5**, 247–248.
34. R. L. K. MATSUMOTO: *J. Am. Ceram. Soc.*, 1987, **70**, (12), C366–C368.
35. M. T. LAUGIER: *J. Mater. Sci. Lett.*, 1987, **6**, 355–356.
36. A. G. EVANS and E. A. CHARLES: *J. Am. Ceram. Soc.*, 1976, **59**, (7–8), 371–372.
37. R. H. MARION: in 'Fracture mechanics applied to brittle materials', STP 678, (ed. S. W. Freiman), 103–111; 1979, Philadelphia, PA, ASTM.
38. B. R. LAWN and E. R. FULLER: *J. Mater. Sci.*, 1975, **10**, 2016–2024.
39. K. TANAKA: *J. Mater. Sci.*, 1987, **22**, 1501–1508.
40. M. K. PETERSSON and B. BERGMAN: *Br. Ceram. Proc.*, 1987, **39**, 15–23.
41. P. LEMAITRE and R. PILLER: *J. Mater. Sci. Lett.*, 1988, **7**, 772–774.
42. N. CLAUSSEN, R. PABST, and C. P. LAHMANN: *Proc. Br. Ceram. Soc.*, 1975, **25**, 139–149.
43. R. F. PABST, K. KROMP, and G. POPP: *Proc. Br. Ceram. Soc.*, 1982, **32**, 89–105.
44. B. MUSSLER, M. V. SWAIN, and N. CLAUSSEN: *J. Am. Ceram. Soc.*, 1982, **65**, (11), 566–572.
45. R. KNEHANS and R. STEINBRECH: in 'Science of ceramics', Vol. 12, 613–619; 1984, Faenza, Ceramurgica.
46. H. WIENINGER, K. KROMP, and R. F. PABST: *J. Mater. Sci.*, 1986, **21**, 411–418.
47. M. V. SWAIN: *J. Mater. Sci. Lett.*, 1986, **5**, 1313–1315.
48. D. B. MARSHALL and A. G. EVANS: *J. Am. Ceram. Soc.*, 1981, **64**, (12), C182–C183.
49. D. B. MARSHALL: *J. Am. Ceram. Soc.*, 1983, **66**, (2), 127–131.
50. A. V. VIRKAR and R. L. K. MATSUMOTO: *J. Am. Ceram. Soc.*, 1986, **69**, (10), C224–C226.
51. E. P. BUTLER: *Mater. Sci. Technol.*, 1985, **1**, 417–432.
52. J. E. BLENDELL: PhD thesis, Massachusetts Institute of Technology, 1979.
53. K. NIIHARA, R. MORENA, and D. P. H. HASSELMAN: *J. Mater. Sci. Lett.*, 1982, **1**, 13–16.
54. J. LANKFORD: *J. Mater. Sci. Lett.*, 1982, **1**, 493–495.
55. D. K. SHETTY and I. G. WRIGHT: *J. Mater. Sci. Lett.*, 1986, **5**, 365–368.
56. M. T. LAUGIER: *J. Mater. Sci. Lett.*, 1985, **4**, 207–210.
57. Y. IKUMA and A. V. VIRKAR: *J. Mater. Sci.*, 1984, **19**, 2233–2238.
58. D. B. MARSHALL and B. R. LAWN: *J. Am. Ceram. Soc.*, 1977, **60**, (1–2), 86–87.
59. D. J. GREEN: *J. Mater. Sci.*, 1985, **20**, 4239–4241.
60. Y. IKUMA and A. V. VIRKAR: *J. Mater. Sci.*, 1985, **20**, 4241–4244.
61. C. B. PONTON and R. D. RAWLINGS: *Br. Ceram. Trans. J.*, 1989, **88**, 83–90.